

ChemMedChem

Supporting Information

Resolving Binding Events on the Multifunctional Human Serum Albumin

Lea Wenskowsky, Michael Wagner, Johannes Reusch, Herman Schreuder, Hans Matter, Till Opatz,* and Stefan Matthias Petry* © 2020 The Authors. Published by Wiley-VCH Verlag GmbH & Co. KGaA. This is an open access article under the terms of the Creative Commons Attribution Non-Commercial NoDerivs License, which permits use and distribution in any medium, provided the original work is properly cited, the use is non-commercial and no modifications or adaptations are made.

Author Contributions

S.P. Conceptualization:Equal; Investigation:Equal; Writing - Original Draft:Equal; Writing - Review & Editing:Equal

L.W. Conceptualization:Equal; Data curation:Equal; Investigation:Lead; Writing - Original Draft:Lead

M.W. Writing - Original Draft:Supporting; Writing - Review & Editing:Equal

J.R. Data curation:Supporting; Investigation:Equal; Writing - Original Draft:Supporting; Writing - Review & Editing:-
Supporting

H.S. Investigation:Equal; Writing - Original Draft:Supporting

H.M. Investigation:Equal; Writing - Original Draft:Supporting; Writing - Review & Editing:Equal

T.O. Conceptualization:Equal; Writing - Original Draft:Equal; Writing - Review & Editing:Equal

Table of Contents

I.	Experimental Procedures	S2
I.I	Material and Methods	S2
I.II	Supplemental Experimental Procedures	S2
I.III	General Information and procedures for biological experiments	S9
II.	Results and Discussion	S12
II.I	Structure solution and refinement	S12
II.II	Supplemental Biochemical Figures	S15
III.	^1H and ^{13}C NMR spectra	S25
IV.	X-Ray crystallization data for BODIPY derivative 5a	S35
V.	Supplemental References	S41
VI.	Author Contribution	S41

I. Experimental Procedures

I.I Materials and Methods

Commercially available reagents, purchased as reagent grade, and acetonitrile (extra dry over molecular sieve, AcroSeal®) were used as received. Dichloromethane was dried over calcium hydride and freshly distilled. All reactions were performed under argon atmosphere. Thin layer chromatography (TLC) was performed with silica gel glass plates (60 F254) and UV light ($\lambda = 254$ nm and $\lambda = 366$ nm) for visualizing the compounds. Flash chromatography for purification was performed on silica gel (40–73 μm). Alternatively, CombiFlash®R_F-system (Teledyne Isco) with a RediSep®R_F column (80 g silica gel, particle size 40–63 μm) was used. A HPLC system with a Sunfire C₁₈ column (50 mm ϕ x 300 mmL, particle size 10 μm) and a micromass ZQ-mass spectrometer from Waters was used for high-performance liquid chromatography (HPLC).

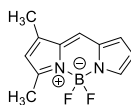
Table S4. HPLC method.

<i>t</i> (min)	B: MeCN (vol%)	flow rate (mLmin ⁻¹)
0	20	30
0–2.9	20	30
2.9–4	20	150
4–24	80	150
24	100	150
24–30	100	150

Melting points were determined in open capillary tubes and are uncorrected. FT-IR-spectra were recorded with a diamond ATR unit. A Q-TOF-instrument with a dual source and a suitable external calibrant were used for high-resolution mass spectra (HRMS). ¹H NMR, ¹³C NMR and ¹⁹F NMR spectra were recorded on a 400 MHz spectrometer (400 MHz for ¹H, 100.6 MHz for ¹³C and 377 MHz for ¹⁹F), a 500 MHz spectrometer (500 MHz for ¹H, 125.6 MHz for ¹³C and 471 MHz for ¹⁹F) and a 600 MHz spectrometer (600 MHz for ¹H and 150.9 MHz for ¹³C). Chemical shifts (δ) were reported in parts per million (ppm) relative to tetramethylsilane (TMS, $\delta = 0.00$ ppm) and referenced to deuterated solvent signals (e.g., for DMSO-*d*₆, $\delta = 2.50$ ppm (¹H) and $\delta = 39.52$ ppm (¹³C); for CDCl₃, $\delta = 7.26$ ppm (¹H) and $\delta = 77.16$ ppm (¹³C); for acetone-*d*₆, $\delta = 2.05$ ppm (¹H) and $\delta = 29.84$ ppm (¹³C); CD₃CN, $\delta = 1.94$ ppm (¹H) and $\delta = 118.26$ ppm (¹³C)).^[1] X-ray crystallography of BODIPY **5a** was performed on a STOE IPDS 2T with Mo-K α radiation and graphite monochromator.

I.II Supplemental Experimental Procedures

1,3-Dimethyl-4,4-difluoro-4-bora-3a,4a-diaza-s-indacene (3)

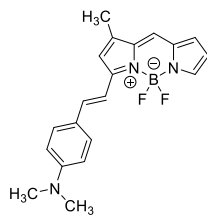


Title compound BODIPY **3** was synthesized according to a procedure reported by Lee et al.^[2]

To a solution of pyrrole-2-carbaldehyde (**2**) (586 mg, 6.16 mmol, 1.0 equiv.) in dry CH₂Cl₂ (10 mL) at -10 °C and under inert atmosphere was added 2,4-dimethylpyrrole (**1**) (349 μL , 6.16 mmol, 1.0 equiv.). The solution was stirred ten minutes and POCl₃ (1.28 mL, 6.16 mmol, 1.0 equiv.) was added dropwise. During three hours the solution was allowed to warm until room temperature. After stirring three hours at room temperature *N,N*-diisopropylethylamine (3.2 mL, 18.5 mmol, 3.0 equiv.) and BF₃·OEt₂ (2.3 mL, 18.5 mmol, 3.0 equiv.) were added. After three hours, the solvent was removed in vacuo. Purification by flash chromatography on silica (n-hexane/EtOAc 8:1) yielded BODIPY **3** (246 mg, 1.12 mmol, 18%) as dark red, green metallic shining solid.

R_f = 0.20 (cyclohexane/EtOAc 10:1). **m. p.**: 141.1–141.9 °C (PE/EtOAc 8:1), (Lit.^[3]): 136–138 °C (PE/EtOAc 10:1). **¹H-NMR, COSY** (300 MHz, CDCl₃): $\delta = 7.64$ (s_{br}, 1H, *H*-7), 7.19 (s, 1H, *H*-8), 6.92 (d, *J*=3.8 Hz, 1H, *H*-5), 6.44–6.41 (m, 1H, *H*-6), 6.15 (s, 1H, *H*-2), 2.59 (s, 3H, CH₃-1), 2.26 (s, 3H, CH₃-3) ppm. The data are in accordance with those reported in the literature.^[2] **¹³C-NMR, HSQC, HMBC** (75.5 MHz, CDCl₃): $\delta = 163.2$ (C_q-8a), 145.9 (C_q-3), 139.3 (CH-7), 136.6 (C_q-1), 132.8 (C_q-7a), 126.6 (CH-5), 124.9 (CH-8), 121.4 (CH-2), 116.4 (CH-6), 15.3 (CH₃-1), 11.5 (CH₃-3) ppm. The data are in accordance with those reported in the literature.^[3] **¹⁹F-NMR** (282 MHz, CDCl₃): $\delta = -147.4$ (q (1:1:1:1), *J*= 31.4 Hz, BF₂) ppm. **IR** (ATR): $\bar{\nu} = 3118, 2925, 2854, 1599, 15293, 1399, 1282, 1264, 1142, 1071, 1032, 971, 738$ cm⁻¹. **HRMS** (ESI): calcd. for C₁₁H₁₁BFN₂ [M-F]⁺ 201.0999; found: 201.0996.

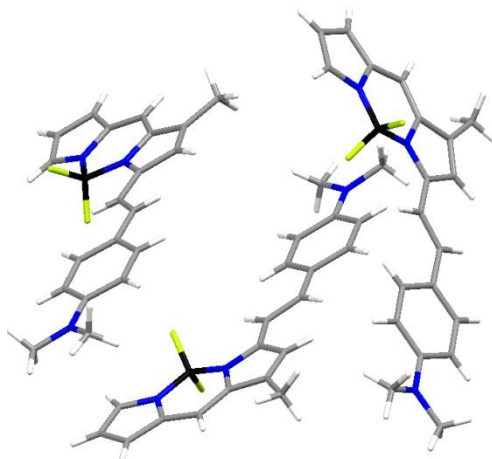
1-Methyl-3-(4-(*N,N*-dimethylamino)styrenyl)-4,4-difluoro-4-bora-3a,4a-diaza-s-indacene (5a)



Title compound **5a** was synthesized according to a procedure reported by *Er et al.*^[4]

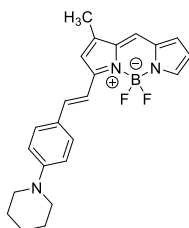
To a solution of BODIPY **3** (25 mg, 0.11 mmol, 1.0 equiv.) in dry acetonitrile (2.5 mL) under inert atmosphere was added acetic acid (39 μ L, 0.66 mmol, 6.0 equiv.) and pyrrolidine (56 μ L, 0.66 mmol, 6.0 equiv.). 4-(Dimethylamino)benzaldehyde (**4a**) (34 mg, 0.22 mmol, 2.0 equiv.) dissolved in acetonitrile (1 mL) was added and the reaction solution was stirred for 25 minutes at 50 °C. The solvent was removed in vacuo. Purification by flash chromatography on silica (cyclohexane/EtOAc 14:1) yielded BODIPY **5a** (32 mg, 92 μ mol, 81%) as dark blue oil.

R_f = 0.21 (cyclohexane/EtOAc 5:1). **¹H-NMR**, COSY (400 MHz, CDCl₃): δ = 7.59 (s_{br}, 1H, *H*-8), 7.54–7.49 (m, 2H, AA'-part of a AA'XX'-spin system, *H*-2', *H*-6'), 7.44 (d, *J* = 16.0 Hz, 1H, BodipyCH=CH), 7.34 (d, *J* = 16.0 Hz, 1H, BodipyCH=CH), 7.03 (s, 1H, *H*-5), 6.82 (d, *J* = 3.8 Hz, 1H, *H*-6), 6.72 (s_{br}, 1H, *H*-2), 6.70–6.65 (m, 2H, XX'-part of a AA'XX'-spin system, *H*-3', *H*-5'), 6.42–6.40 (m, 1H, *H*-7), 3.04 (s, 6H, N(CH₃)₂), 2.27 (s, 2H, CH₃-1) ppm. **¹³C-NMR**, HSQC, HMBC (100.6 MHz, CDCl₃): δ = 144.8 (C_q-7a), 161.0 (C_q-3), 152.1 (C_q-4'), 142.3 (BodipyCH=CH), 138.8 (C_q-8a), 136.7 (CH-8), 133.0 (C_q-1), 130.5 (CH-2', CH-6'), 124.3 (C_q-1'), 123.9 (C_q-6), 120.9 (CH-5), 117.9 (CH-2), 115.7 (CH-7), 113.9 (BodipyCH=CH), 112.4 (CH-3', CH-5'), 40.6 (N(CH₃)₂), 11.9 (CH₃-1) ppm. **¹⁹F-NMR** (296 MHz, CDCl₃): δ = -144.0 (q (1:1:1:1), *J* = 31.6 Hz, BF₂) ppm. **IR** (ATR): $\bar{\nu}$ = 3068, 2920, 2857, 1583, 1524, 1398, 1287, 1149, 1160, 1028, 725 cm⁻¹. HRMS (ESI): calcd. for [C₂₀H₂₀BF₂N₃Na]⁺ 374.1616; found: 374.1627.



The accession number for this X-ray crystal structure of BODIPY derivative **5a** is CCDC 1917091.

1-Methyl-3-(4-(piperidin-1-yl)styrenyl)-4,4-difluoro-4-bora-3a,4a-diaza-s-indacene (5b)

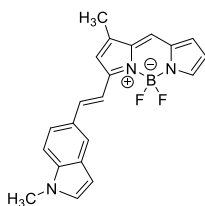


Title compound **3** was synthesized according to a procedure reported by *Er et al.*^[4]

To a solution of BODIPY **3** (25 mg, 0.11 mmol, 1.0 equiv.) in dry acetonitrile (2.5 mL) under inert atmosphere was added acetic acid (39 μ L, 0.66 mmol, 6.0 equiv.) and pyrrolidine (56 μ L, 0.66 mmol, 6.0 equiv.). 4-(Piperidin-1-yl)benzaldehyde (**4b**) (43 mg, 0.22 mmol, 2.0 equiv.) dissolved in acetonitrile (1 mL) was added and the reaction solution was stirred for 20 minutes at 40 °C. The solvent was removed in vacuo. Purification by flash chromatography on silica (*n*-hexane/EtOAc 8:1 + 1% NEt₃) yielded BODIPY **5b** (23 mg, 59 μ mol, 52%) as dark blue, metallic shining oil.

$R_f = 0.25$ (cyclohexane/EtOAc 5:1). **¹H-NMR, COSY** (400 MHz, CDCl₃): $\delta = 7.61$ (s_{br}, 1H, *H*-8), 7.53–7.49 (m, 2H, AA'-part of a AA'XX'-spin system, *H*-2', *H*-6'), 7.46 (d, $J = 16.2$ Hz, 1H, BodipyCH=CH), 7.34 (d, $J = 16.2$ Hz, 1H, BodipyCH=CH), 7.06 (s, 1H, *H*-5), 6.90–6.86 (m, 2H, XX'-part of a AA'XX'-spin system, *H*-3', *H*-5'), 6.84 (d, $J = 3.9$ Hz, 1H, *H*-6), 6.74 (s_{br}, 1H, *H*-2), 6.43–6.40 (m, 1H, *H*-7), 3.35–3.31 (m, 4H, 2×N(CH₂)), 2.29 (s, 3H, CH₃-1), 1.73–1.62 (m, 6H, 3×CH₂) ppm. **¹³C-NMR, HSQC, HMBC** (100.6 MHz, CDCl₃): $\delta = 160.6$ (C_q-3), 153.0 (C_q-4'), 144.7 (C_q-7a), 141.6 (BodipyCH=CH), 138.6 (C_q-8a), 137.1 (CH-8), 133.0 (C_q-1), 130.2 (CH-2', CH-6'), 125.7 (C_q-1'), 124.2 (CH-6), 121.2 (CH-5), 117.7 (CH-2), 115.8 (CH-7), 115.1 (CH-3', CH-5'), 114.7 (BodipyCH=CH), 49.3 (2×N(CH₂)), 25.7 (3×CH₂), 11.8 (CH₃-1) ppm. **¹⁹F-NMR** (471 MHz, CDCl₃): $\delta = -142.6$ (q (1:1:1:1), $J = 31.2$ Hz, BF₂) ppm. **IR** (ATR): $\bar{\nu} = 2961, 2928, 2360, 1730, 1592, 1523, 1397, 1289, 1126, 1072, 957$ cm⁻¹. **HRMS** (ESI): calcd. for [C₂₃H₂₅BF₂N₃]⁺ 392.2108; found: 392.2116.

1-Methyl-3-(2-(1-methylindol-5-yl)ethenyl)-4,4-difluoro-4-bora-3a,4a-diaza-s-indacene (5c)

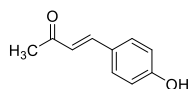


Title compound **5c** was synthesized according to a procedure reported by *Er et al.*^[4]

To a solution of BODIPY **3** (25 mg, 0.11 mmol, 1.0 equiv.) in dry acetonitrile (2.5 mL) under inert atmosphere was added acetic acid (39 μ L, 0.66 mmol, 6.0 equiv.) and pyrrolidine (56 μ L, 0.66 mmol, 6.0 equiv.). 1-Methyl-1*H*-indole-5-carbaldehyde (**4c**) (36 mg, 0.22 mmol, 2.0 equiv.) dissolved in dry acetonitrile (1 mL) was added and the reaction solution was stirred for 3 hours at 40 °C. The solvent was removed in vacuo. Purification by CombiFlash®R_f-system on silica (*n*-heptane/EtOAc, 5% EtOAc (60 min), then 15% EtOAc (20 min)) yielded BODIPY **5c** (18 mg, 50 μ mol, 44%) as dark blue, metallic shining oil.

$R_f = 0.25$ (cyclohexane/EtOAc 4:1). **¹H-NMR, COSY** (400 MHz, CDCN₃): $\delta = 7.86$ (d, $J = 1.6$ Hz, 1H, *H*-4'), 7.78 (d, $J = 16.3$ Hz, 1H, BODIPYCH=CH), 7.59 (s_{br}, 1H, *H*-8), 7.56 (dd, $J = 8.7$ Hz, $J = 1.6$ Hz, 1H, *H*-6'), 7.52 (d, $J = 16.3$ Hz, 1H, BODIPYCH=CH), 7.48–7.43 (m, 1H, *H*-7'), 7.40 (s, 1H, *H*-5), 7.22 (d, $J = 3.2$ Hz, 1H, *H*-2'), 6.98 (s, 1H, *H*-6), 6.97 (s_{br}, 2H, *H*-2), 6.55 (dd, $J = 3.2$ Hz, $J = 0.8$ Hz, 1H, *H*-3'), 6.49–6.45 (m, 1H, *H*-7), 3.81 (s, 3H, N(CH₃)), 2.33 (s_{br}, 3H, CH₃-1) ppm. **¹³C-NMR, HSQC, HMBC** (100.6 MHz, CDCN₃): $\delta = 161.4$ (C_q-3), 147.1 (C_q-7a), 144.8 (BODIPYCH=CH), 139.3 (C_q-8a), 139.0 (C_q-7a'), 137.7 (CH-8), 133.7 (C_q-1), 131.9 (CH-2'), 130.0 (C_q-3a'), 128.2 (C_q-5'), 125.7 (CH-6), 123.7 (CH-5), 123.3 (CH-4'), 121.8 (CH-6'), 118.6 (CH-2), 116.7 (CH-7), 115.5 (BODIPYCH=CH), 111.4 (CH-7'), 102.8 (CH-3'), 33.4 (N(CH₃)), 11.7 (CH₃-1) ppm. **¹⁹F-NMR** (377 MHz, CDCN₃): $\delta = -143.1$ (q (1:1:1:1), $J = 31.4$ Hz, BF₂) ppm. **IR** (ATR): $\bar{\nu} = 2924, 2853, 1596, 1524, 1416, 1312, 1287, 1145, 1063, 994$ cm⁻¹. **HRMS** (ESI): calcd. for [C₂₁H₁₈BF₂N₃Na]⁺ 384.1460; found: 384.1463.

(3E)-4-(4-Hydroxyphenyl)but-3-en-2-one (7a)



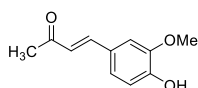
Title compound **7a** was synthesized according to the procedure reported by *Chen et al.*^[5]

To a solution of 4-hydroxybenzaldehyde (**6a**) (1.22 g, 9.99 mmol, 1.0 equiv.) in acetone (15 mL) was added an aqueous solution of sodium hydroxide (10%, 25 mL). The reaction mixture was stirred for 24 h at room temperature and then acidified to pH 1 with an aqueous solution of HCl (10%). The aqueous phase was extracted with dichloromethane (3 × 30 mL). The combined organic layers were washed with brine (30 mL), dried over Na₂SO₄ and filtered. The solvent was removed in vacuo. Purification by flash chromatography on silica (cyclohexane/EtOAc 4:1) yielded product **7a** (1.33 g, 8.20 mmol, 82%) as yellowish solid.

$R_f = 0.35$ (cyclohexane/EtOAc 2:1). **m.p.**: 102.1–104.8 °C (cyclohexane/EtOAc 2:1), (Lit.^[5]): 109 °C (*n*-hexane/EtOAc 5:1). **¹H-NMR, COSY** (300 MHz, DMSO-*d*₆): $\delta = 10.04$ (s_{br}, 1H, OH), 7.55–7.51 (m, AA'-part of a AA'XX'-part spin system, 2H, *H*-2, *H*-6), 7.52 (d, $J = 16.3$ Hz, 1H, ArCH=CH), 6.84–6.78 (m, XX-part of a AA'XX'-part spin system, 2H, *H*-3, *H*-5), 6.59 (d, $J = 16.3$ Hz, 1H, ArCH=CH), 2.28 (s, 3H, CH₃) ppm. In the literature the data are available in CDCl₃.^[5] **¹³C-NMR, HSQC, HMBC** (75.5 MHz, DMSO-*d*₆): $\delta = 197.8$ (CO), 159.9 (C_q-4), 143.6 (ArCH=CH), 130.4 (CH-2, CH-6), 125.4 (C_q-1), 124.1 (ArCH=CH), 115.9 (CH-3, CH-5), 27.2 (CH₃) ppm. In the literature the data are available in CDCl₃.^[5] **HRMS** (ESI): calcd. for [C₁₀H₁₁O₂]⁺ 163.0759; found: 163.0769.

¹ Signals for C_q-7a and C_q-8a could not be assigned without a doubt.

(3E)-4-(4-Hydroxy-3-methoxyphenyl)but-3-en-2-one (**7b**)

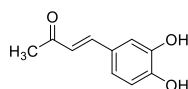


Title compound **7b** was synthesized according to the procedure reported by *Chen et al.*^[5]

To a solution of 4-hydroxy-3-methoxybenzaldehyde (**6b**) (1.01 g, 6.64 mmol, 1.0 equiv.) in acetone (10 mL) was added an aqueous solution of sodium hydroxide (10%, 17 mL). The reaction mixture was stirred for 3 h at room temperature and then acidified to pH 1 with an aqueous solution of HCl (10%). The aqueous phase was extracted with dichloromethane (3 x 30 mL). The combined organic layers were washed with brine (30 mL), dried over Na₂SO₄ and filtered. The solvent was removed in vacuo. Purification by flash chromatography on silica (cyclohexane/EtOAc 5:1→3:1) yielded **7b** (910 mg, 5.16 mmol, 71%) as yellowish solid.

R_f = 0.29 (cyclohexane/EtOAc 2:1). **m.p.**: 125.3–126.6 °C (cyclohexane/EtOAc 5:1), (Lit.^[5]): 127–128 °C (*n*-hexane/EtOAc 10:1). **¹H-NMR, COSY** (300 MHz, DMSO-*d*₆): δ = 9.65 (s, 1H, OH), 7.52 (d, J = 16.3 Hz, 1H, ArCH=CH), 7.30 (d, J = 1.9 Hz, 1H, *H*-2), 7.13 (dd, J = 8.20 Hz, J = 1.9 Hz, 1H, *H*-6), 6.82 (d, J = 8.1 Hz, 1H, *H*-5), 6.67 (d, J = 16.3 Hz, 1H, ArCH=CH), 3.82 (s, 3H, OCH₃), 2.29 (s, 3H, CH₃) ppm. In the literature the data are available in CDCl₃.^[5] **¹³C-NMR, HSQC, HMBC** (75.5 MHz, DMSO-*d*₆): δ = 197.9 (CO), 149.4 (C_q-4), 148.0 (C_q-3), 144.0 (ArCH=CH), 125.9 (C_q-1), 124.4 (ArCH=CH), 123.3 (CH-6), 115.7 (CH-5), 111.3 (CH-2), 55.7 (OCH₃), 27.2 (CH₃) ppm. In the literature the data are available in CDCl₃.^[5]

(3E)-4-(3,4-Dihydroxyphenyl)but-3-en-2-one (**7c**)

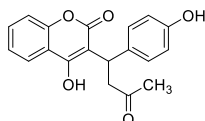


Title compound **7c** was synthesized according to a procedure reported by *Chen et al.*^[5]

An aqueous solution of sodium hydroxide (10%, 36 mL) was added to a solution of 3,4-dihydroxybenzaldehyde (**6c**) (2.00 g, 14.5 mmol, 1.0 äq.) in acetone (15 mL). The reaction mixture was stirred for 3 h at room temperature and then acidified to pH 1 with an aqueous solution of HCl (10%). The aqueous phase was extracted with dichloromethane (3 x 100 mL). The combined organic layers were washed with brine (100 mL), dried over MgSO₄ and filtered. The solvent was removed in vacuo. The crude product was purified by flash chromatography on silica (cyclohexane/EtOAc 2:1) to yield the product **7c** (2.15 g, 12.1 mmol, 83%) as a yellow solid.

R_f = 0.71 (EtOAc/EtOH/H₂O 17:2:1). **m.p.**: 172.0–174.1 °C (cyclohexane/EtOAc 3:2), (Lit.^[6]): 173–175 °C (*n*-hexane/EtOAc). **¹H-NMR** (300 MHz, acetone-*d*₆): δ = 7.47 (d, J = 16.2 Hz, 1H, ArCH=CH), 7.17 (d, J = 2.1 Hz, 1H, *H*-2), 7.06 (dd, J = 8.2 Hz, J = 2.1 Hz, 1H, *H*-6), 6.87 (d, J = 8.2 Hz, 1H, *H*-5), 6.54 (d, J = 16.2 Hz, 1H, ArCH=CH), 2.27 (s, 3H, CH₃) ppm. The data are in accordance with those reported in the literature.^[7] **¹³C-NMR** (75.5 MHz, acetone-*d*₆): δ = 197.7 (CO), 148.6 (C_q-4), 146.2 (C_q-3), 144.1 (ArCH=CH), 127.9 (C_q-1), 125.3 (ArCH=CH), 122.7 (CH-6), 116.4 (CH-5), 115.2 (CH-2), 27.3 (CH₃) ppm. The data are in accordance with those reported in the literature.^[7]

3-[1-(4-Hydroxyphenyl)-3-oxobutyl]-4-methyl-2H-chromen-2-one (**8a**)



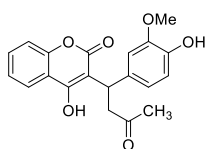
Title compound **8a** was synthesized according to a procedure reported by *Halland et al.*^[8]

4-Hydroxy-2H-chromen-2-one (106 mg, 0.65 mmol, 1.05 eq.) was dissolved in DMSO (4.8 mL). l-proline (36 mg, 0.31 mmol, 0.5 eq.) and (3E)-4-(4-hydroxyphenyl)but-3-en-2-one (**7a**) (91 mg, 0.62 mmol, 1.0 eq.) were added and the reaction solution was stirred for 3 days at room temperature. Diethyl ether (20 mL) and water (10 mL) were added and the aqueous phase was extracted with diethyl ether (4 x 10 mL). The combined organic layers were washed with water (10 mL), dried over Na₂SO₄ and filtered. The solvent was removed in vacuo. The crude product was purified by flash chromatography on silica (cyclohexane/EtOAc 2:1, then toluene/EtOAc 3:1) to yield an isomeric mixture of **8a** (77 mg, 238 μ mol, 42%) as yellowish solid.

R_f = 0.42 (cyclohexane/EtOAc 1:1). **m.p.**: 208.5–209.9 °C (chloroform). **IR** (ATR): $\tilde{\nu}$ = 3363, 2924, 2853, 1693, 1614, 1515, 1455, 1390, 1237, 1072, 763 cm⁻¹. **HRMS** (ESI): calcd. for [C₁₉H₁₆O₅Na]⁺ 347.0895; found: 347.0887.

Table S5. ¹H-NMR signals (600 MHz, acetone-d₆) and ¹³C (150.9 MHz, acetone-d₆) of hemiacetals **8aA–B**.

Atom number	¹ H hemiacetal 8aA	¹ H hemiacetal 8aB	¹³ C hemiacetal 8aA	¹³ C hemiacetal 8aB
C _q -1	-	-	160.9	161.4
C _q -2	-	-	105.5	103.8
C _q -3	-	-	159.2	159.9
C _q -4	-	-	117.1	116.9
5	7.84	7.85	123.6	123.7
6	7.33	7.35	124.4	124.5
7	7.58	7.61	132.3	132.5
8	7.27	7.29	116.9	117.0
C _q -9	-	-	153.86	153.88
10	4.02	4.02	35.8	36.5
11 (CH ₂ -A)	2.39	2.39	44.0	42.6
11 (CH ₂ -B)	2.00	2.28	-	-
C _q -12	-	-	100.3	101.9
OH-12	6.22	5.89	-	-
C _q -14	-	-	135.6	135.3
15	7.05	7.07	129.0	129.3
16	6.73	6.70	115.9	115.7
C _q -17	-	-	156.5	156.4
OH-17	8.02	7.99	-	-
CH ₃	1.71	1.66	28.0	26.6

3-[1-(4-Hydroxy-3-methoxyphenyl)-3-oxobutyl]-4-methyl-2H-chromen-2-one (8b)

Title compound **8b** was synthesized according to a procedure reported by *Halland et al.*^[8]

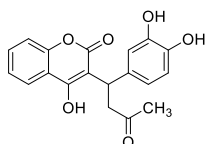
4-Hydroxy-2H-chromen-2-one (1.69 g, 10.4 mmol, 1.05 eq.) was dissolved in DMSO (25 mL). l-proline (572 mg, 4.97 mmol, 0.5 eq.) and (3E)-4-(4-hydroxy-2-methoxyphenyl)but-3-en-2-one (**7b**) (1.91 g, 9.93 mmol, 1.0 eq.) were added and the reaction solution was stirred for 3 days at room temperature. Diethyl ether (40 mL) and water (20 mL) were added and the aqueous phase was extracted with diethyl ether (3 × 50 mL). The combined organic layers were washed with water (50 mL), dried over Na₂SO₄ and filtered. The solvent was removed in vacuo. The crude product was purified by flash chromatography on silica (cyclohexane/EtOAc 3:1, then toluene/EtOAc 3:1→1:1, then toluene/EtOAc 3:1) to yield an isomeric mixture of product **8b** (2.08 g, 5.87 mmol, 59%) as colourless solid.

R_f = 0.36 (cyclohexane/EtOAc 1:1). **m.p.**: 126.8–129.6 °C (cyclohexane/EtOAc 1:1), (Lit.^[9]): 181 °C (EtOH). **IR** (ATR): $\tilde{\nu}$ = 3384, 2934, 2850, 1686, 1618, 1515, 1454, 1382, 1239, 1073, 762 cm⁻¹. **HRMS** (ESI): calcd. for [C₂₁H₁₉O₆]⁺ 355.1182; found: 355.1172.

Table S6. ¹H-NMR signals (600 MHz, acetone-d₆) and ¹³C (150.9 MHz, acetone-d₆) of hemiacetals **8bA–B**.

Atom number	¹ H hemiacetal 8bA	¹ H hemiacetal 8bB	¹³ C hemiacetal 8bA	¹³ C hemiacetal 8bB
C _q -1	-	-	161.0	161.4
C _q -2	-	-	105.4	103.7
C _q -3	-	-	159.2	159.9
C _q -4	-	-	117.1	116.9
5	7.84	7.78	123.65	123.68
6	7.33	7.35	124.3	124.5
7	7.58	7.60	132.3	132.5
8	7.26	7.29	116.9	117.0
C _q -9	-	-	153.85	153.88
10	4.02	4.03	36.2	37.0
11 (CH ₂ -A)	2.40	2.40	43.9	42.6
11 (CH ₂ -B)	2.04	2.31	-	-
C _q -12	-	-	100.3	101.9
OH-12	6.30	5.98	-	-
C _q -14	-	-	136.3	136.0
15	6.87	6.90	111.9	112.3
C _q -16	-	-	148.2	148.0
C _q -17	-	-	145.7	145.7
18	6.71	6.68	115.6	115.4
19	6.66	6.68	120.5	120.7
OCH ₃	3.77	3.75	56.2	56.2
CH ₃	1.72	1.66	28.0	26.5

3-[1-(3,4-Dihydroxyphenyl)-3-oxobutyl]-4-methyl-2H-chromen-2-one (**8c**)



Title compound **8c** was synthesized according to a procedure reported by *Halland et al.*^[8]

4-Hydroxy-2H-chromen-2-one (1.64 g, 10.1 mmol, 1.05 eq.) was dissolved in DMSO (24 mL). l-proline (556 mg, 4.83 mmol, 0.5 eq.) and (3E)-4-(3,4-dihydroxyphenyl)but-3-en-2-one (**7b**) (1.72 g, 9.65 mmol, 1.0 eq.) were added and the reaction solution was stirred for 3 days at room temperature. Diethyl ether (40 mL) and water (20 mL) were added and the aqueous phase was extracted with diethyl ether (4 × 25 mL). The combined organic layers were washed with water (50 mL), dried over Na₂SO₄ and filtered. The solvent was removed in vacuo. The crude product was purified by flash chromatography on silica (cyclohexane/EtOAc 1:2) and by HPLC (see table 2) to yield an isomeric mixture of **8b** (287 mg, 842 μmol, 9%) as yellowish solid.

R_f = 0.79 (EtOAc/EtOH/H₂O 17:2:1). **m.p.**: 115.7–118.1 °C (MeCN/H₂O, 80/20). **IR** (ATR): $\tilde{\nu}$ = 3348, 2927, 2855, 1681, 1612, 1519, 1447, 1390, 1073, 736 cm⁻¹. **HRMS** (ESI): calcd. for [C₁₉H₁₇O₆]⁺ 341.1020; found: 341.1019.

Table S7. ¹H-NMR signals (600 MHz, acetone-d₆) and ¹³C (150.9 MHz, acetone-d₆) of hemiacetals **7cA–B**.

Atom number	¹ H hemiacetal 8cA	¹ H hemiacetal 8cB	¹³ C hemiacetal 8cA	¹³ C hemiacetal 8cB
C _q -1	-	-	160.9	161.4
C _q -2	-	-	105.5	103.8
C _q -3	-	-	159.1	159.8
C _q -4	-	-	117.1	116.9
5	7.84	7.86	123.6	123.7
6	7.33	7.35	124.4	124.5
7	7.59	7.61	132.3	132.5
8	7.27	7.30	116.9	117.0
C _q -9	-	-	153.8	153.9
10	3.96	3.98	35.9	36.5
11 (CH ₂ -A)	2.39	2.39	44.0	42.6
11 (CH ₂ -B)	1.99	2.29		
C _q -12	-	-	100.4	102.0
OH-12	6.20	5.78	-	-
C _q -14	-	-	136.6	136.2
15	6.68	6.71	115.2	115.4
C _q -16	-	-	145.7	145.6
C _q -17	-	-	144.2	144.1
18	6.71	6.69	116.0	115.9
19	6.57	6.60	119.5	119.6
CH ₃	1.71	1.65	28.0	26.5

I.III General Information and protocols for biochemical assays

Human serum albumin was purchased as lyophilized and fatty acid free ($\leq 0.007\%$) from Sigma Aldrich (A1887). Warfarin (**2**), iophenoxic acid (**3**), ketoprofen (**4**), indomethacin (**5**), ibuprofen (**1**), semaglutide, and liraglutide were commercially available. Stock solutions (10 mM) of **1–5**, **8a–c** were prepared in ethanol. The BODIPY dyes **5a–c** were dissolved in ethanol at 2.5 mM. Sulfasalazine (**6**) and balsalazide (**7**) were dissolved in PBS (800 μM , max. 5 vol% DMSO). Dulbecco's phosphate-buffered saline (PBS (1X), no calcium, no magnesium, Gibco[®], Scotland) containing KCl, NaCl, KH_2PO_4 , and $\text{Na}_2\text{HPO}_4 \cdot 7\text{H}_2\text{O}$ (pH 7.08) was used for stock solutions of HSA (100 μM). All stock solutions were stored at 4–5 °C. Under this storage conditions HSA solutions can be used for 2 days. Required concentrations were diluted with PBS. The HSA concentration was determined by optical density using the photometer NanoDrop with molar excitation coefficient (ϵ) $\epsilon(280) = 32810 \text{ M}^{-1}\text{cm}^{-1}$.^[10] All described experiments were performed at 20 °C. The microplate reader Varioskan[™] (Thermo Scientific) was used for recording the spectroscopic data in black 96 well half area microplates from Greiner Bio-One (see wavelengths for every dye in table 1). Absorption spectra were recorded on a Evolution 201 photometer from Thermo Scientific. Fluorescence spectra were measured on a FP-8300 fluorometer from Thermo Scientific. Analysis was performed with GraphPad Prism^[11] (version 7.0). Standard errors were calculated as SEM. The abbreviations c (μM) (concentration in micro molar), F (AU) (fluorescence intensity, arbitrary unit), and χ_{HSA} (substance amount fraction of human serum albumin) were used for the axes of diagrams. The pH values were determined using the pH meter Titrino Plus 877 from Metrohm.

Table S1. Excitation and emission wavelengths for each dye.

Compound	Excitation wavelength (λ_{ex})	Emission wavelength (λ_{em})
NBD-FA	435 nm	535 nm
Coumarin 8a	330 nm	384 nm
Coumarin 8b	326 nm	380 nm
Coumarin 8c	330 nm	384 nm
BODIPY 5a	615 nm	690 nm
BODIPY 5b	615 nm	678 nm
BODIPY 5c	554 nm	600 nm

Absorption and fluorescence spectra

For the spectra of BODIPY **5a–c**, warfarin derivatives **8a–c** and of warfarin (**2**) 2 mL of a 40 μM solution of the ligand was pipetted into a fluorescence cuvette and analysed.

Fluorescence titration

A clear microplate (Greiner Bio one, 384 well flat bottom) was prepared with the HSA solution (35 μL) and with a 1:1 ratio the serial dilutions of the ligand (see final concentrations in the figure description) were transferred into it and mixed 6 times. An aliquot (50 μL) of each HSA/ligand solution was taken after 30 minutes and analysed. For each concentration and for the control four replicates were performed. The final concentration of the HSA solution is 25 μM for the warfarin derivatives **8a–c** and 12.5 μM for the BODIPY dyes **5a–c**.

Job Plots

Binding stoichiometries were measured according to the method described by Job and Huang.^[12-13] The substance amount fraction of HSA was varied with a total volume of 70 μL (see the final concentration in the figure description) and pipetted into a clear microplate (Greiner Bio one, 384 well flat bottom). The solutions were mixed 6 times and after 30 minutes the fluoroscopic measurements were done. For each concentration and for the control three replicates were performed.

One-dye competition experiments

The one-dye/HSA complex solution (1:1 ratio) was prepared at 20 °C and used after 20 minutes. A clear microplate (Greiner Bio one, 384 well flat bottom) was filled with 35 μL of the dye/HSA solution and with a 1:1 ratio the serial dilutions of the ligand were pipetted into it and mixed 6 times. After 30 minutes an aliquot (50 μL) of each solution was taken and analysed. The final concentration for the warfarin derivatives **8a–c** is 25 μM . Competition experiments with the BODIPY dyes **5a–c** were performed at a concentration of 12.5 μM .

Three-dye competition assay

The three-dye/HSA complex solution (16 μM each dye, 50 μM HSA, each final) was prepared at 20 °C and used after 20 minutes. A clear microplate (Greiner Bio one, 384 well flat bottom) was prepared with 35 μL of the three-dye/HSA complex solution and with a 1:1 ratio the serial dilutions of the ligand were pipetted into it and mixed 6 times. An aliquot of 50 μL of each three-dye/HSA/ligand solution was taken after 30 minutes and analysed. For each concentration and for the control four replicates were performed.

Biosensor Experiments

Measurements were performed on a switchSENSE® DRX² instrument (Dynamic Biosensors, Germany) using a biochip (MPC-48-2-R2-S, Dynamic Biosensors) where ligands are tethered to a gold microelectrode via short DNA strands (48 bp, 16nm). One strand of the DNA duplex is covalently attached to the surface via Au-S bonds and carries a fluorescent dye at the top end while the complementary strand can be functionalized with a molecule of interest (ligand) via *in vitro* coupling chemistry. switchSENSE® features two complementary measurement modes. In static measurement mode (fluorescence proximity sensing, FPS) the DNA strands are repelled from the surface (constant voltage, $V_{\text{att}} = V_{\text{rep}} = -0.1 \text{ V}$). For signal detection of biomolecular interactions the fluorescence intensity of the dye is read out. It changes its fluorescence emission when static or collisional quenching by bound complexes occurs. The fluorescence signal change is proportional to the surface bound analytes. In the molecular dynamic mode DNA strands are oscillated by applying alternating potentials ($f = 10 \text{ kHz}$, $V_{\text{att}} = +0.5 \text{ V}$; $V_{\text{rep}} = -0.3 \text{ V}$), and thereby the change in hydrodynamic friction when analyte molecules bind to surface-immobilized ligands is determined.

The measurement principle of the switchSENSE® technology is based on electro-switchable DNA strands. Core Element of the technology is a biochip featuring up to 20 electrodes in four flow channels. Short DNA double strands are attached to each gold microelectrode (100 μm in diameter). One single strand of the DNA double helix is covalently attached to the gold surface via gold sulfur bonds whereas the upper end features a fluorescent dye as readout. The complementary DNA strand can be functionalized (*in vitro*) with a target of interest (immobilized ligand). If an analyte (in solution) is rinsed over the flow channel and captured by the ligand the fluorescent dye is used as readout. Therefore, the switchSENSE® technology features mainly two different measurement modes which generate complementary information content. In the molecular dynamics mode short DNA nanolevers attached to the gold surface are altered by a potential (AC potential). As there are alternating voltages applied the negatively charged DNA is repeatedly attracted and repelled from the gold surface with frequencies up to 10 kHz. Whenever the DNA is in close proximity to the gold surface by applying a positive voltage the emission of the fluorescent dye is quenched. When the analyte binds to a ligand attached to the DNA its hydrodynamic friction is changed, slowing down the DNA movement. The motion of the complex is recorded in real-time by single photon counting. Depending on the interplay of bound complex (ligand and analyte), its shape and size, the switching speed of the complex is changed in a characteristic way. The bigger the complex, the slower it moves due to increasing of hydrodynamic friction. The systems software uses the friction change upon binding for the calculation of absolute and relative sizes (hydrodynamic radius) as well as kinetics (Langer). Analyzing the DNA movement (switching speed) allows insights into the absolute hydrodynamic radius of ligands attached to the DNA as well as conformational changes upon analyte binding. Conformational change modelling using the switchSENSE software package knowing crystal structures can be used to confirm the identity of binding partners, stoichiometry, and multimeric binding. By detecting the binding of an analyte in real-time the molecular dynamic mode can also be used to measure binding rate constants (k_{ON} , k_{OFF}) and the dissociation constant (K_{D}). Au Contraire, the second measurement mode, the Fluorescence Proximity Sensing (static mode) is size independent. It measures real-time kinetics recording fluorescent dye changes occurring in molecular environment upon analyte binding. There is no AC potential applied. Since this measurement mode is nearly size and buffer independent it is very suitable for the detection of small molecule / inhibitor binding to a protein / nucleic acid of interest.

Surface Functionalization

A switchSENSE® multi-purpose chip with 48bp DNA strands (MPC-48-2-R2-S, Dynamic Biosensors) was used for all experiments. Single stranded DNA is covalently attached to the gold microelectrode and carries a red fluorescence dye at the top end (3' end) for signal detection while the complementary strand is exchangeable and can be functionalized with different molecules. Following the instruction manual of the thiol reactive protein-DNA coupling kit (CK-SH-1-B48, Dynamic Biosensors), HSA was site-specifically attached to the maleimide-functionalized 5' end of a complementary 48 nt single-stranded DNA *in vitro* via its free cysteine residue. After the purification of the HSA-DNA conjugate using anion exchange chromatography (proFIRE, Dynamic Biosensors), the sample was aliquoted and stored in PE140 buffer (10 mM $\text{Na}_2\text{HPO}_4/\text{NaH}_2\text{PO}_4$, 140 mM NaCl, 50 μM EDTA, 50 μM EGTA and 0.05 % Tween 20, pH 7.4; 0.2 μm sterile filtered) at -80°C. For the automated surface functionalization 100 nM HSA-DNA conjugate were incubated on the microelectrode for 10 minutes prior to the kinetics measurement. To ensure full surface saturation, the hybridization kinetics was observed in real-time.

Assay Design

All measurements were performed in PE140 buffer with 1% DMSO. For kinetics and equilibrium experiments, the static measurement mode was used. Conformational change studies were measured in the molecular dynamic mode and with a compound concentration of tenfold higher than the respective K_{D} value for the specific interaction. The kinetics measurements were performed at a flow rate of 2 mL/min with a sampling rate of 10 Hz to resolve the fast kinetics rate constants.

X-Ray diffraction data collection and structure determination Crystallization

Essentially defatted human serum albumin from Sigma was purified by size exclusion chromatography to obtain pure monomeric protein.^[14] The purified HSA was dissolved in 20 mM potassium phosphate (pH 7.0) and concentrated to 2 mM (140 mg/mL). The HSA solution was incubated with an eight-fold excess of sulfasalazine at 4–5 °C for 24 hours. The final concentration of dimethyl sulfoxide was 5% (v/v). The crystal was grown by the hanging drop vapor diffusion method using a reservoir solution containing buffer (50 mM sodium-potassium-phosphate (pH 7.0), and 24.5% polyethylene glycol 3350). For crystallization, 1 μ L of HSA/sulfasalazine solution was equilibrated against 1 μ L of reservoir solution. After about one week, colorless crystals appeared

Data collection and processing

For cryoprotection, the nylon loop was wetted with glycerol and the crystal was picked directly from the crystallization drop and immediately flash frozen in liquid nitrogen.

X-ray diffraction data were collected at beamline PX-III of the Swiss Light Source (SLS) in Villigen, Switzerland, and processed with XDS^[15] and scaled with Aimless^[16] and STARANISO^[17] as implemented in autoProc.^[18] The crystal was of space group $P2_1$ and contained one HSA molecule in the asymmetric unit. The unit cell dimensions of this crystal are as follows: $a = 59.3$, $b = 85.1$ and $c = 60.2$ Å with $\beta = 99.9^\circ$.

The diffraction was anisotropic and for this reason we used anisotropic scaling. The crystal diffracted to 2.2 Å resolution in the direction of the $-a^*, +c^*$ diagonal, but only to 2.8 Å resolution in the direction of the $+a^*, +c^*$ diagonal. Rmerge was 6.6%. Final data collection and refinement statistics are given in Table S2 (Section Results and Discussion).

II. Results and Discussion

II.I Structure solution and refinement

The structure was determined by molecular replacement using the program Phaser,^[19] using the pdb structure 4s1y as search model. Model building was done with Coot^[20] and refinement was done with Buster^[21] using default settings. The electron density for the loop 77-88 was very weak and this loop could not be modeled. Otherwise, the HSA molecule fits the electron density map quite well. The final model contains residues 5-76 and 89-583 and has the same conformation as the search model 4s1y.^[22]

We observed difference density for three bound sulfasalazine molecules; one at the expected position near the indole group of Trp214 in Sudlow site I, one in domain IIIb and one at the interface between domains IIIa and IIIb. Whereas the first sulfasalazine molecule, fitted in drug side one, has reasonably strong electron density for the whole molecule, the second ligand molecule in domain IIIb has weaker density and almost no density for the pyridine ring, probable due to rotational disorder around the phenyl-sulfonyl bond and, finally, the third ligand molecule at the interface between domains IIIa and IIIb has reasonably strong electron density for the hydroxybenzoate group, but weak density for the remaining parts of the molecule, probably since these parts are somewhat disordered.

After more refinement final structure was obtained with an Rfactor of 17.9% and a free Rfactor of 27.9%. The free Rfactor is high, which might be due to a certain amount of disorder in our crystals as evidenced by the strong anisotropy of our data.

Table S2. Crystallographic Data Collection and Refinement Statistics.

PDB code	PDB ID 6R7S				
Data collection					
Space group name	P2 ₁				
Unit cell parameters	59.297	85.11	60.12	90.000	99.889 90.000
Wavelength	1.00000 Å				
Diffraction limits & eigenvectors of ellipsoid fitted to diffraction cut-off surface:					
2.830	0.7189	0.0000	0.6951	0.784 <i>_a_*</i> + 0.621 <i>_c_*</i>	
2.563	0.0000	1.0000	0.0000	<i>_b_*</i>	
2.157	-0.6951	0.0000	0.7189	-0.638 <i>_a_*</i> + 0.770 <i>_c_*</i>	
			Overall	Inner Shell	Outer Shell
Low resolution limit			48.616	48.616	2.473
High resolution limit			2.208	7.094	2.208
<i>R_{merge}</i> (all I+ & I-)			0.066	0.020	0.729
<i>R_{merge}</i> (within I+/-)			0.056	0.017	0.612
<i>R_{meas}</i> (all I+ & I-)			0.078	0.024	0.861
<i>R_{meas}</i> (within I+/-)			0.078	0.023	0.850
<i>R_{pim}</i> (all I+ & I-)			0.042	0.013	0.453
<i>R_{pim}</i> (within I+/-)			0.054	0.016	0.589
Total number of observations			62922	3166	3270
Total number unique			18420	921	922
Mean(I)/sd(I)			12.7	47.9	1.6
Completeness (spherical)			62.1	98.9	10.8
Completeness (ellipsoidal)			90.1	98.9	59.5
Multiplicity			3.4	3.4	3.5
CC(1/2)			0.999	0.999	0.600
Refinement					
protein atoms:			4434		
ligand atoms:			84		
water atoms:			333		
resolution (Å)			48.62-2.21	(2.38-2.21)*	
<i>R_{work}</i> (%)			17.9	(22.2)	
<i>R_{free}</i> (%)			27.2	(28.4)	
average Bfactors (Å ²)					
protein:			54.14		
ligand:			51.20		
water:			47.37		
rmsd bond lengths (Å)			0.010		
rmsd bond angles (°)			1.14		

* The highest resolution bin is given in brackets

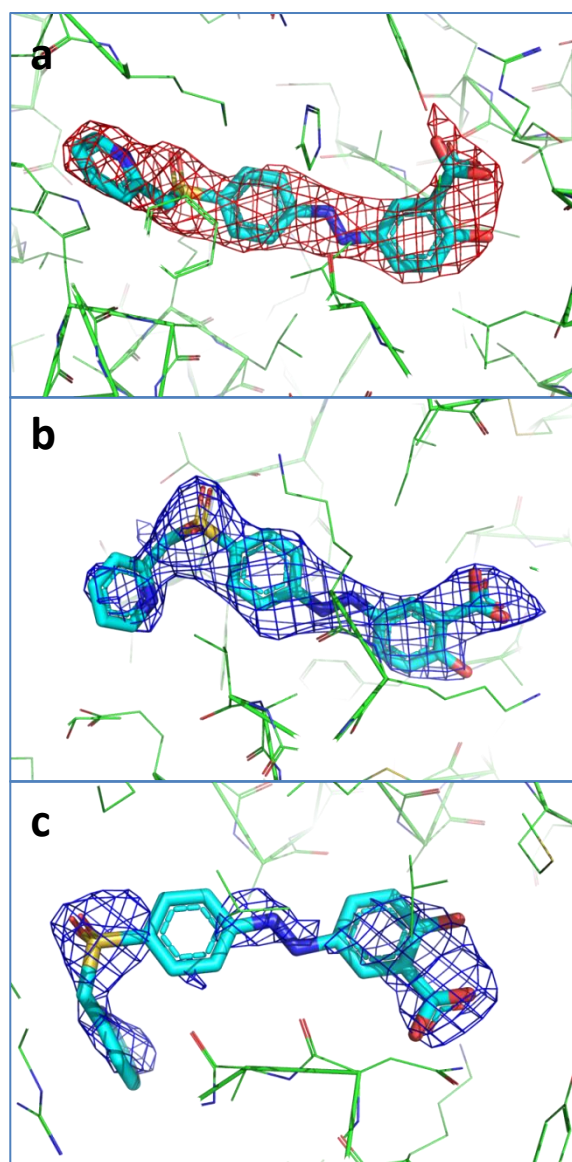


Figure S1. Omit map of the bound sulfasalazine molecules, contoured at 3σ (a) or 2σ (b,c). a) Primary binding site in drug site 1. b) Secondary binding site in domain IIIb. c) Tertiary binding site at the interface of domains IIIa and IIIb. The molecule bound in drug site 1 has stronger omit electron density than the 2 other molecules.

Since it is known that the free Cys34 in commercial HSA preparations may be partially oxidized we examined Cys34 in our electron density maps, but did not find evidence for oxidation. While this might be difficult to detect in our anisotropic somewhat disordered electron density maps, we did not detect oxidation in a 1.76 Å crystal structure of HSA with a proprietary compound prepared from HSA from the same source either. We therefore believe that the oxidation of Cys34, if any, will be minor and will not distort the crystal structure obtained.

Crude estimate of the K_D of the binding sites

We refined group occupancies for all three bound molecules, listed in table S3. From the occupancies, we can calculate the concentration of bound ligand $[PL] = \text{occupancy} \times \text{total HSA}$; the concentration of free binding site $[P] = \text{total HSA} - [PL]$ and $[L] = \text{total ligand} - \text{sum}[PL]$. Using the formula $K_d = [P][L]/[PL]$ we get the K_d values listed in the table. The K_d measured for sulfasalazine in our biochemical assay's was 218 μM . These calculations show that the first binding site (drug site 1) is the high affinity binding site.

Table S3. Crude estimation of K_D based on fractional occupancies.

[HSA]	[Ligand]	occupancy	[P]	[L]	[PL]	K_D
2	16	0.92	0.16	10.92	1.84	0.9
2	16	0.86	0.28	10.92	1.72	1.8
2	16	0.76	0.48	10.92	1.52	3.4

[HSA] = total HSA concentration; [Ligand] = total ligand concentration;

[P] = concentration of free binding site; [L] = free ligand concentration;

[PL] = occupied binding site concentration. All concentrations and K_D 's are in mM.

A computational analysis of hydration sites in the HSA subdomain IIA binding site of the sulfasalazine complex reveal that displacement of those hydration sites with appropriate energetics is related to ligand affinity and indicates important ligand-protein interactions. This analysis of hydration sites was done using WaterMap^[23] from a 2 ns MD simulation. Figure 2A summarizes WaterMap derived hydration sites from a simulation without ligand mapped onto the HSA/sulfasalazine complex. For visualization, only hydration sites within 4 Å of the ligand are displayed. In fact, the ligand replaces energetically unfavorable (brown-red) hydration sites next to its salicylate, the sulfonamide, the linker and the distal pyridine ring. More favorable (green) hydration sites are located at the central phenyl ring. A comparison of ligand binding modes bound to HSA subdomain IIA from protein superposition only is shown in Figure 2F for sulfasalazine R/S warfarin and NBD-FA.

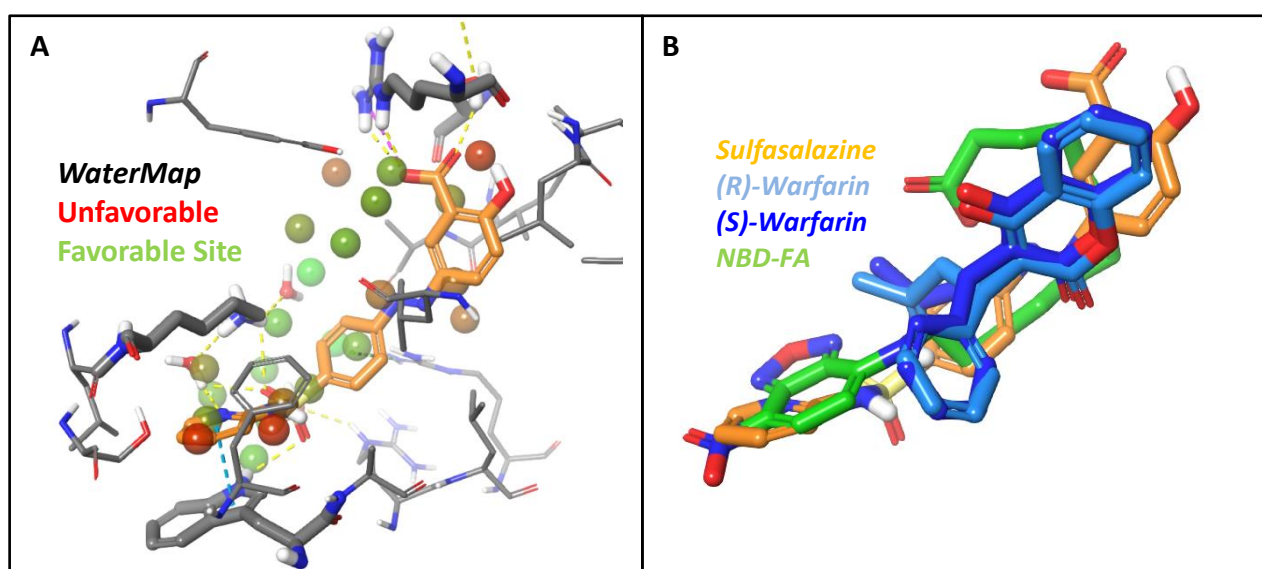


Figure S2. A) WaterMap hydration sites from 2 ns MD simulation mapped onto the binding mode of sulfasalazine in HSA subdomain IIA. All hydration sites within 4 Å around the bound ligand are displayed to illustrate energetically unfavorable and favorable sites. Green spheres indicate stable hydration sites with more negative ΔG values; red-brown spheres indicate more positive ΔG values, i.e. more instable sites. B) Comparison of ligand binding modes for sulfasalazine (orange), (R)-warfarin (light-blue), (S)-warfarin (dark-blue) and NBD-FA (green carbon atoms) binding to HSA subdomain IIA.

II.II Supplemental Biochemical Figures

Characterization of BODIPY derivatives 5b–c and warfarin derivatives 8b–c

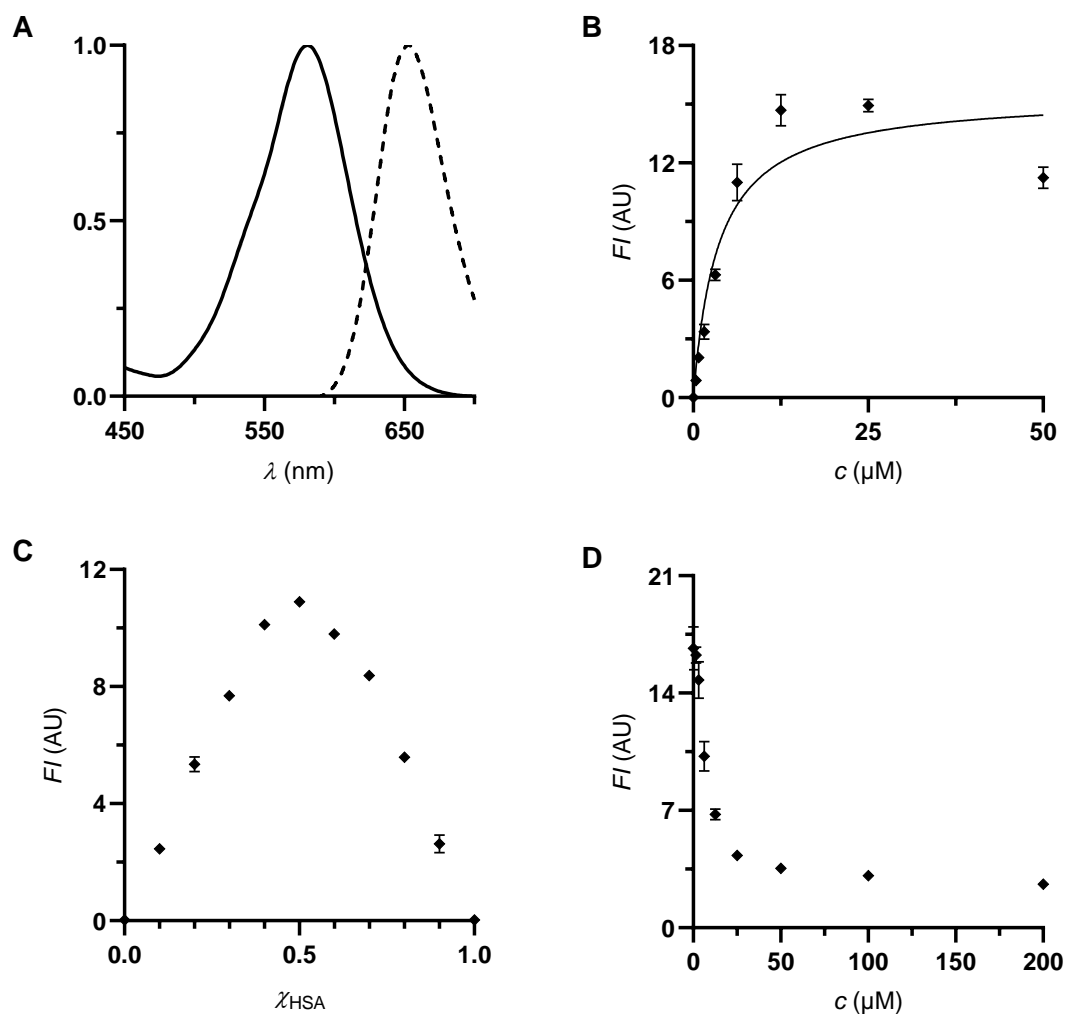


Figure S3. A) Absorption and emission spectra (both normalized) of piperidinyl-BODIPY **5b** (40 μM ethanol). $\lambda_{\text{exc}} = 581$ nm. B) Titration of piperidinyl-BODIPY **5b** (0–50 μM) to HSA (12.5 μM in PBS pH 7.4) ($K_{\text{D}} = 3.6 \pm 0.7$ μM . $R^2 = 0.8927$). C) Determination of the binding stoichiometry of piperidinyl-BODIPY **5b** to HSA (12.5 μM , Job plot). D) Competition experiment of ibuprofen (1) against piperidinyl-BODIPY **5b** on HSA (12.5 μM each).

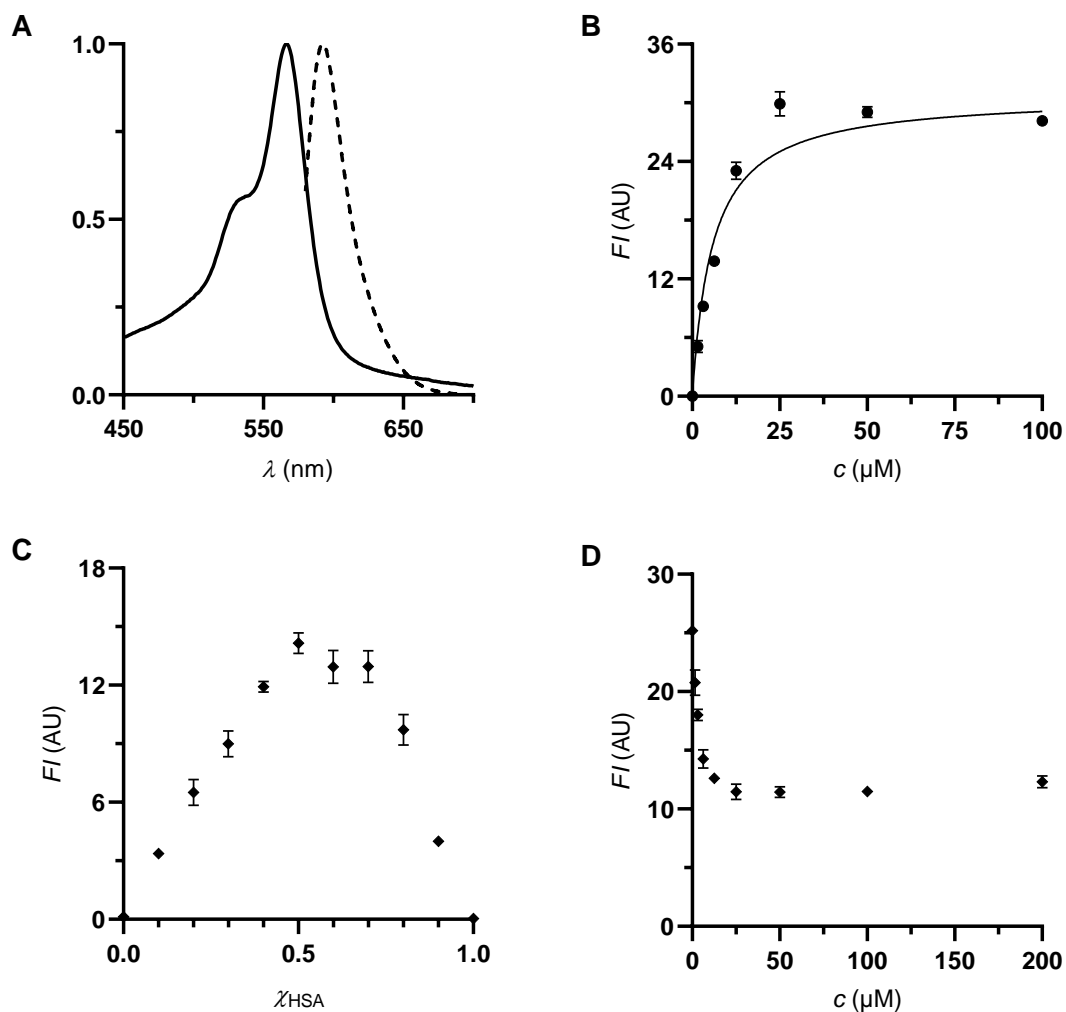


Figure S4. A) Absorption and emission spectra (both normalized) of indolyl-BODIPY 5c (40 μM ethanol). $\lambda_{\text{exc}} = 567$ nm. B) Titration of indolyl-BODIPY 5c (0–50 μM) to HSA (12.5 μM) ($K_D = 5.8 \pm 0.8$ μM , $R^2 = 0.9363$). C) Determination of the binding stoichiometry of indolyl-BODIPY 5c to HSA (12.5 μM , Job plot). D) Competition experiment of ibuprofen (1) against indolyl-BODIPY 5c on HSA (12.5 μM each).

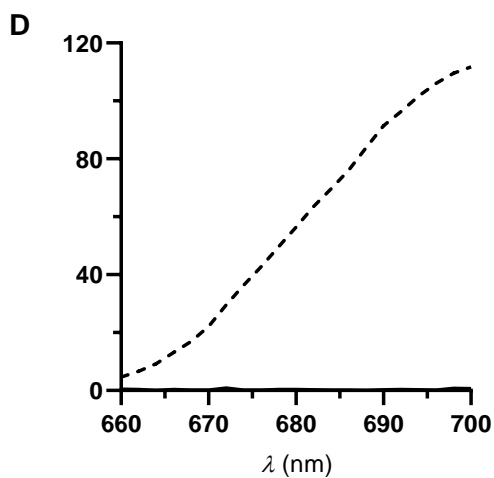


Figure S5. A) Emission spectrum of warfarin (2) with HSA (dashed) and without HSA. $\lambda_{\text{exc}} = 615$ nm.

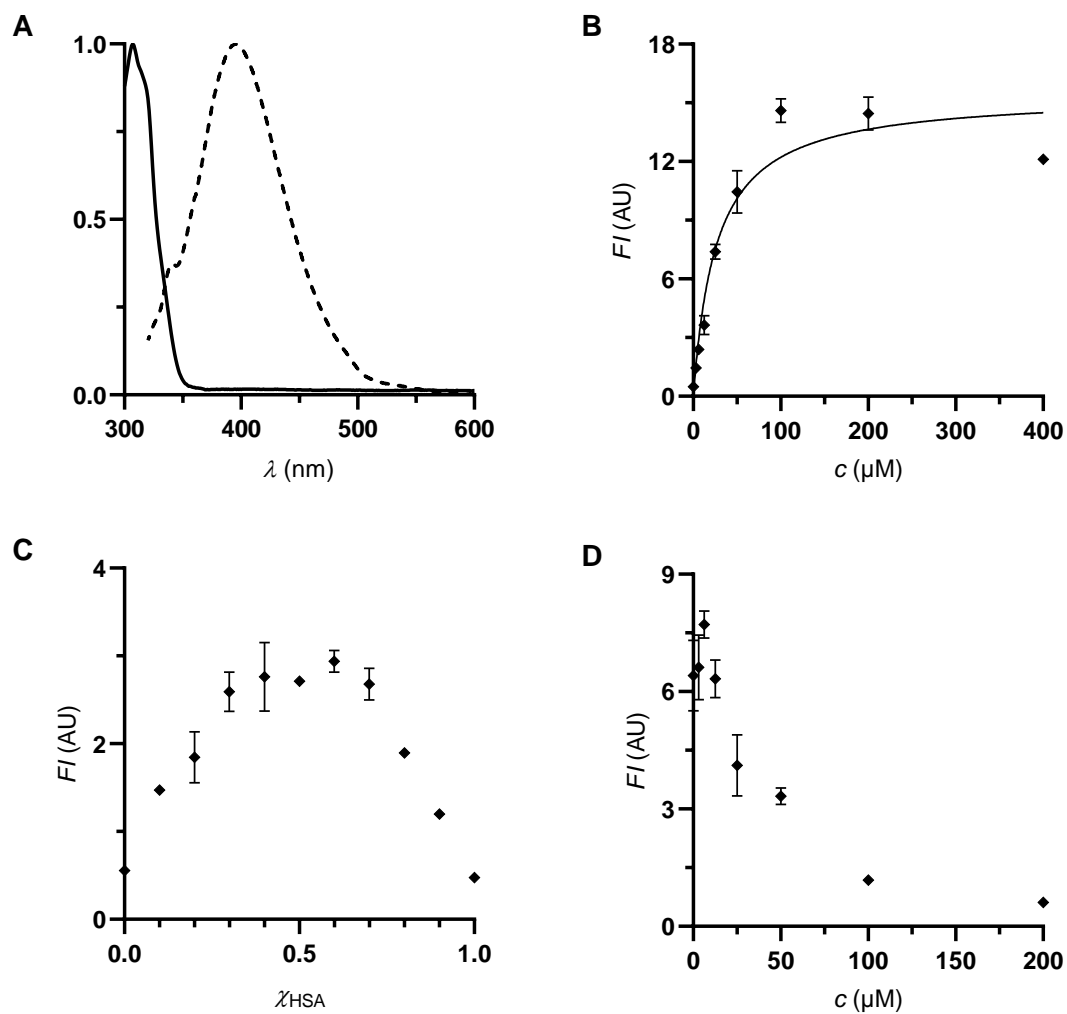


Figure S6. A) Absorption and emission spectra (both normalized) of warfarin derivative **8b** (40 μM ethanol). $\lambda_{\text{exc}} = 307$ nm. B) Titration of warfarin derivative **8b** (0–400 μM) to HSA (25 μM) ($K_D = 26.5 \pm 4.5$ μM , $R^2 = 0.9150$). C) Determination of the binding stoichiometry of warfarin derivative **8b** to HSA (25 μM , Job plot). D) Competition experiment of iopexic acid (**3**) against warfarin derivative **8b** on HSA (25 μM each).

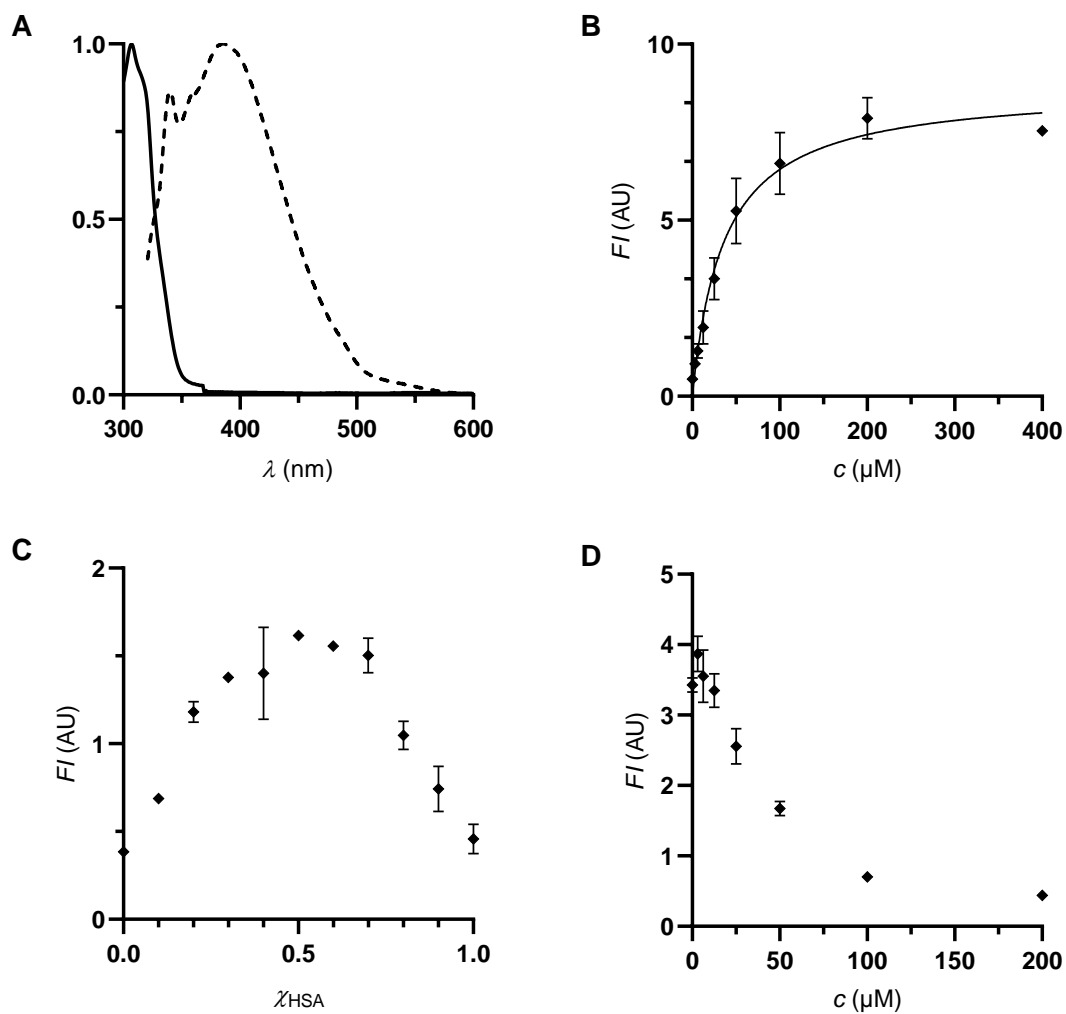


Figure S7. A) Absorption and emission spectra (both normalized) of warfarin derivative **5a** (40 μM ethanol). $\lambda_{\text{exc}} = 307$ nm. B) Titration of warfarin derivative **5a** (0–400 μM) to HSA (25 μM) ($K_D = 36.3 \pm 7.2$ μM , $R^2 = 0.8862$). C) Determination of the binding stoichiometry of warfarin derivative **5a** to HSA (25 μM , Job plot). D) Competition experiment of iophenoxic acid (**3**) against warfarin derivative **5a** on HSA (25 μM each).

Biosensor experiments

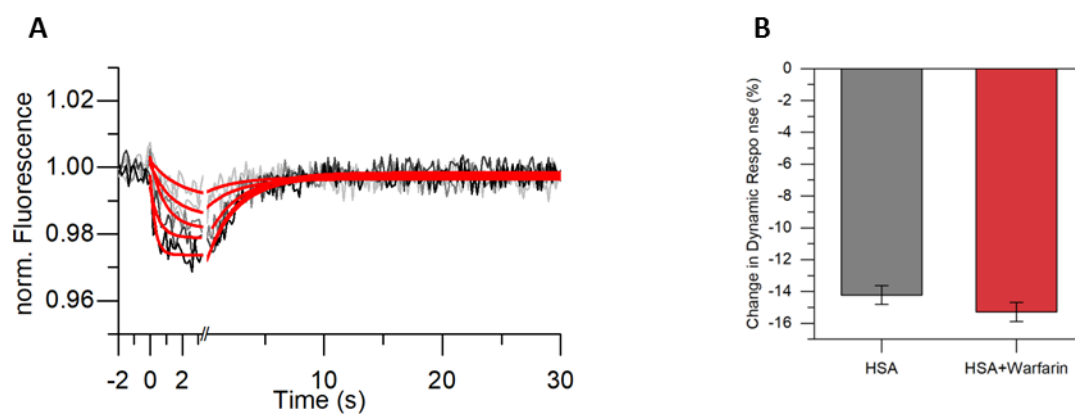


Figure S8. A) Kinetic investigation of warfarin derivative **8a** using switch sense Technology (proximity sensing, $n = 3$, Data average per concentration, 5 concentrations $12.5 \mu\text{M} - 200 \mu\text{M}$). B) Relative size analysis of HSA in presence of $200 \mu\text{M}$ **8a** reveals no change of hydrodynamic diameter.

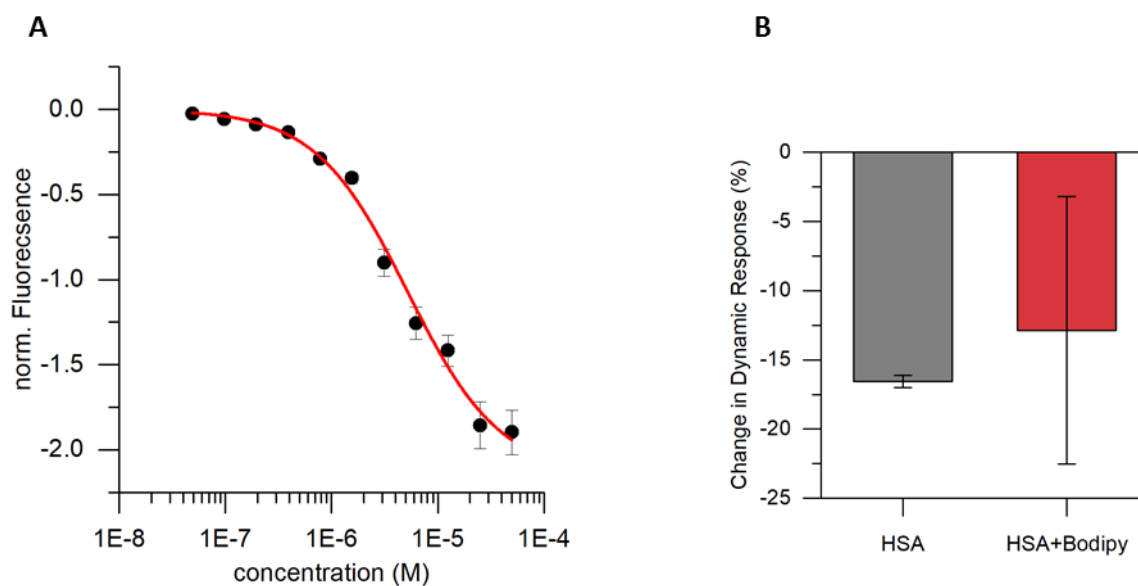


Figure S9. A) Kinetic investigation BODIPY derivative **5a** using switch sense Technology. B) Relative size analysis of HSA in presence of $400 \mu\text{M}$ **5a** causes no significant change in hydrodynamic diameter.

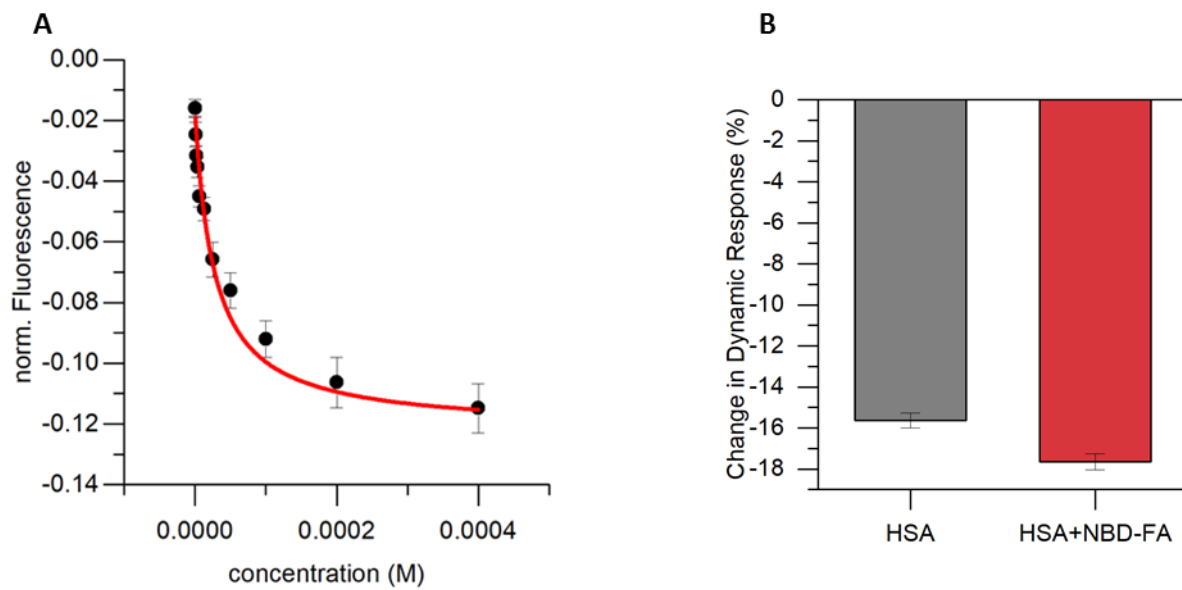


Figure S10. A) Kinetic investigation NBD-FA using switch sense Technology. B) Relative size analysis of HSA in presence of 400 μM NBD-FA causes a slight but significant HSA expansion of hydrodynamic diameter.

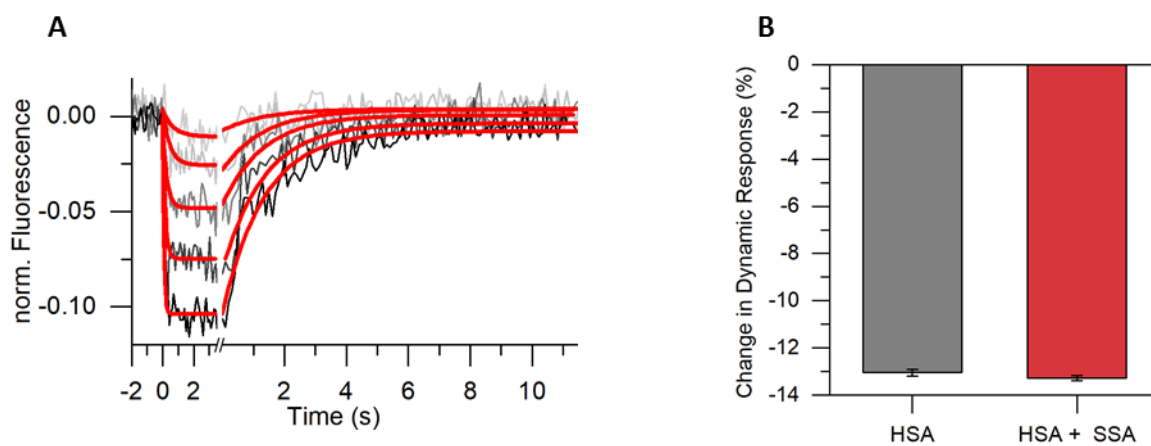


Figure S11. A) Kinetic investigation of sulfasalazine (**6**, SSA) using switch sense Technology. B) Relative size analysis of HSA in presence of 20 μM sulfasalazine (**6**) causes no significant change in hydrodynamic diameter.

Competition experiments against BODIPY derivative 5a

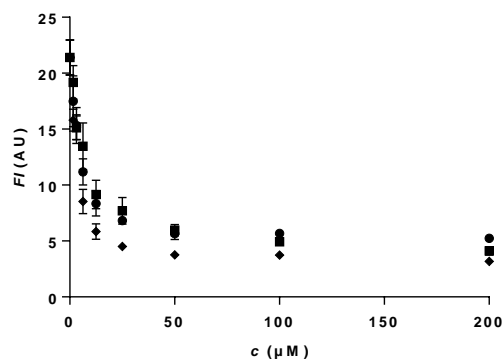


Figure S12. Competition experiment of ibuprofen (●), ketoprofen (■) and naproxen (◆) against dimethylamino-BODIPY **5a** on HSA (12.5 μM each). $\lambda_{exc} = 615$ nm. $\lambda_{em} = 690$ nm.

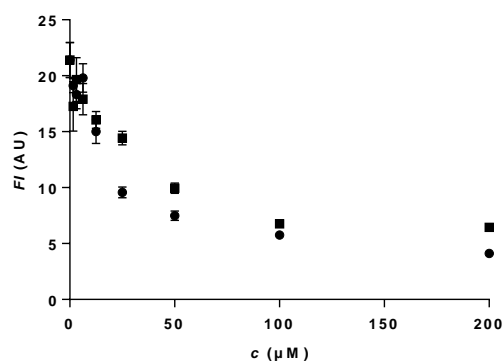


Figure S13. Competition experiment of myristic acid (●) and myristic acid methyl ester (■) against dimethylamino-BODIPY **5a** on HSA (12.5 μM each). $\lambda_{exc} = 615$ nm. $\lambda_{em} = 690$ nm.

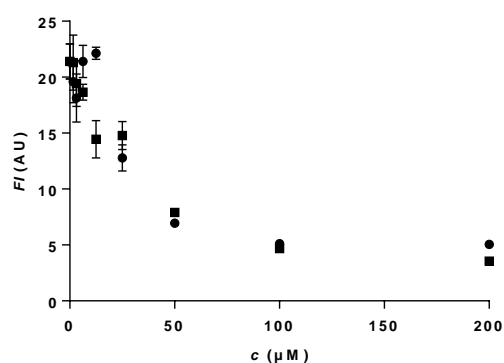


Figure S14. Competition experiment of iophenoxic acid (●) and indomethacin (■) against dimethylamino-BODIPY **5a** on HSA (12.5 μM each). $\lambda_{exc} = 615$ nm. $\lambda_{em} = 690$ nm.

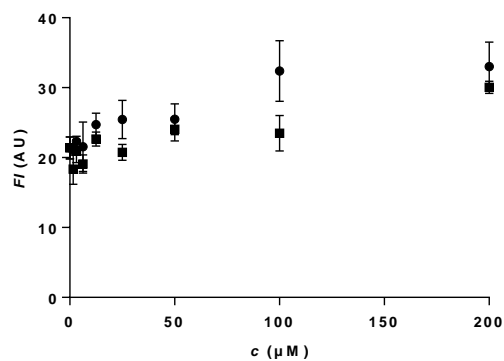


Figure S15. Competition experiment of sulfasalazine (●) and balsalazide (■) against dimethylamino-BODIPY **5a** on HSA (12.5 μM each). $\lambda_{exc} = 615$ nm. $\lambda_{em} = 690$ nm.

Competition experiments against coumarin **8a**

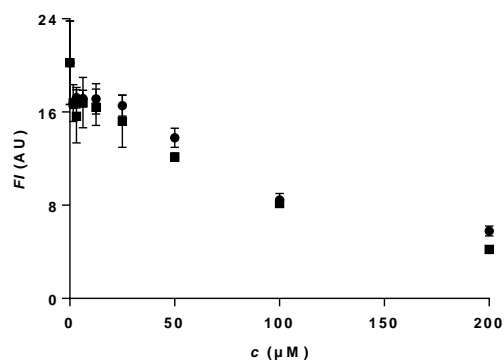


Figure S16. Competition experiment of ibuprofen (●) and ketoprofen (■) against warfarin-derivative **8a** on HSA (25 μM each). $\lambda_{exc} = 330$ nm. $\lambda_{em} = 384$ nm.

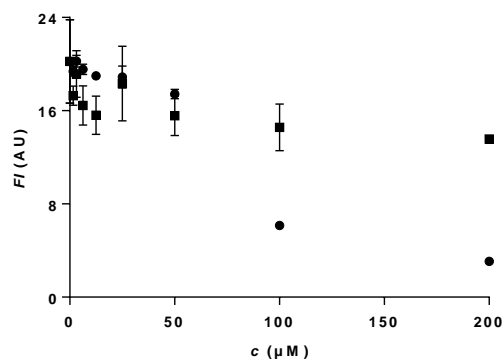


Figure S17. Competition experiment of myristic acid (●) and myristic acid methyl ester (■) against warfarin-derivative **8a** on HSA (25 μM each). $\lambda_{exc} = 330$ nm. $\lambda_{em} = 384$ nm.

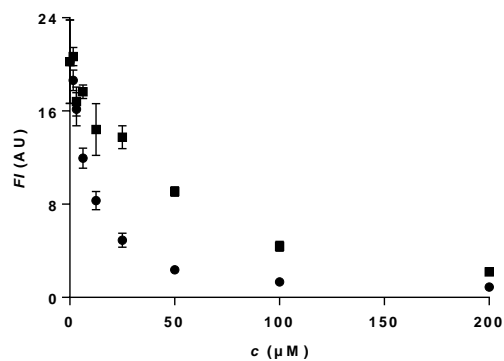


Figure S18. Competition experiment of iophenoxic acid (●) and indomethacin (■) against warfarin-derivative **8a** on HSA (25 μM each). $\lambda_{exc} = 330$ nm. $\lambda_{em} = 384$ nm.

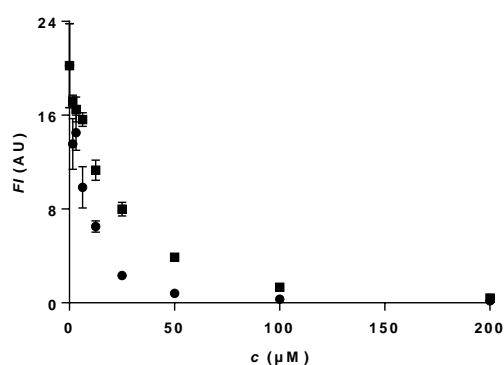


Figure S19. Competition experiment of sulfasalazine (●) and balsalazide (■) against warfarin-derivative **8a** on HSA (25 μM each). $\lambda_{exc} = 330$ nm. $\lambda_{em} = 384$ nm.

Competition experiments of fatty acid modified GLP1 agonists

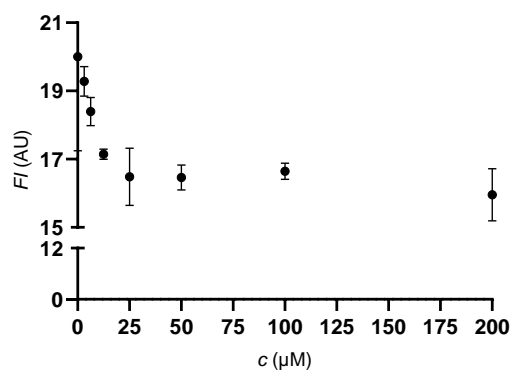


Figure S20. Competition experiment of liraglutide against NBD-FA on HSA (25 μM each). $\lambda_{exc} = 435$ nm. $\lambda_{em} = 535$ nm.

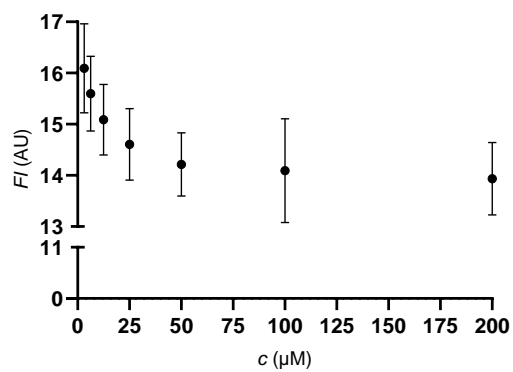


Figure S21. Competition experiment of semaglutide against NBD-FA on HSA (25 μM each). $\lambda_{exc} = 435$ nm. $\lambda_{em} = 535$ nm.

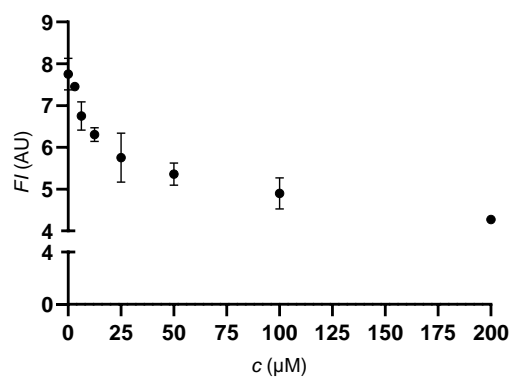


Figure S22. Competition experiment of semaglutide against dimethylamino-BODIPY 5a on HSA (12.5 μM each). $\lambda_{exc} = 615$ nm. $\lambda_{em} = 690$ nm.

III. ^1H and ^{13}C NMR spectra

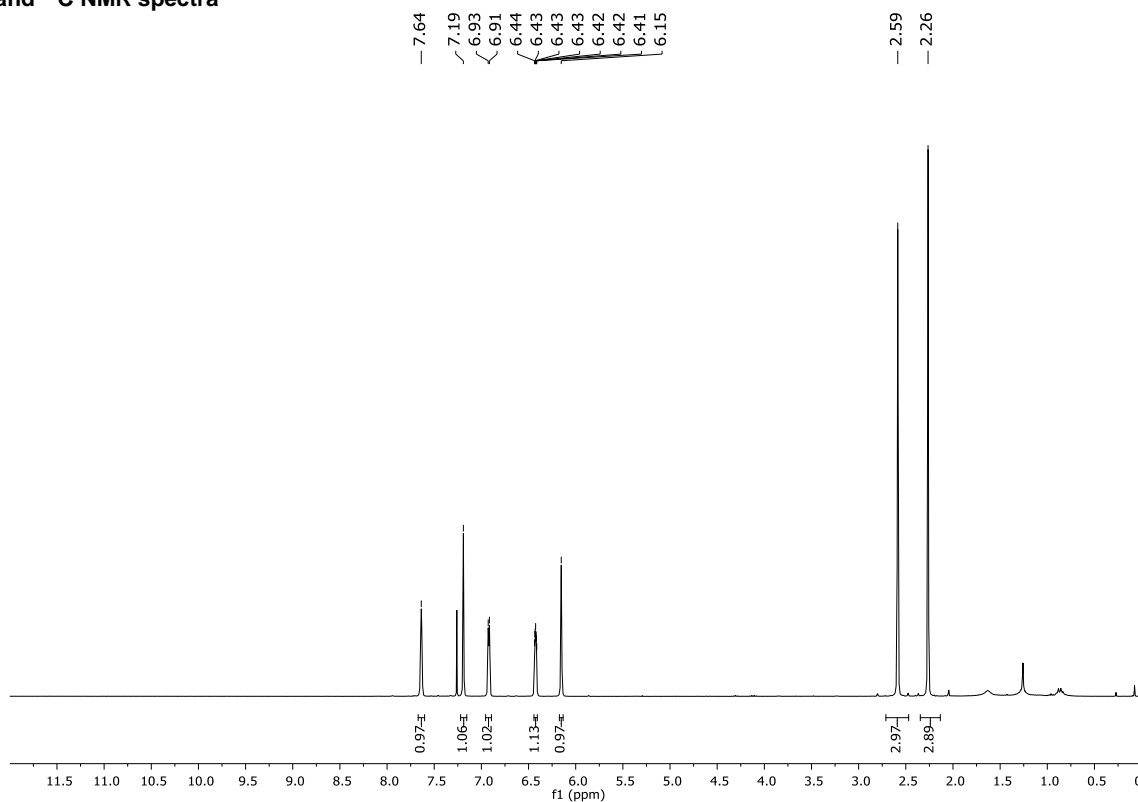


Figure S23. BODIPY 3: ^1H -NMR (300 MHz, CDCl_3).

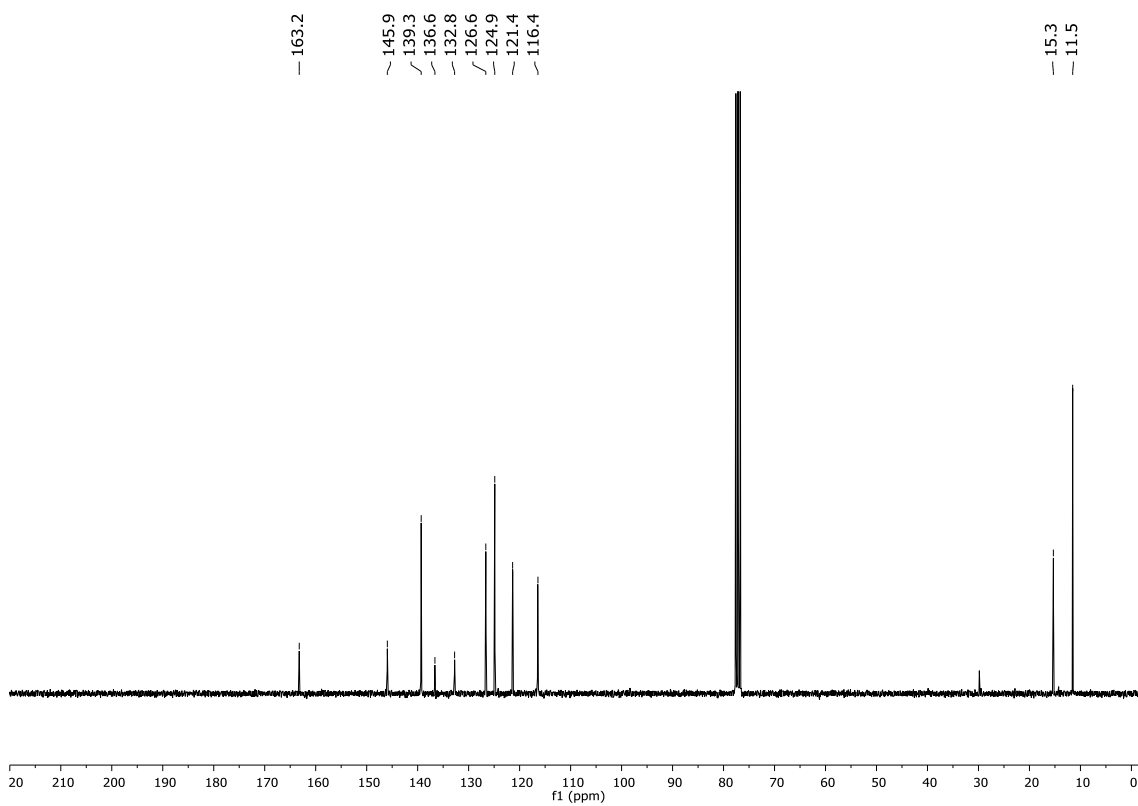


Figure S24. BODIPY 3: ^{13}C -NMR (75.5 MHz, CDCl_3).

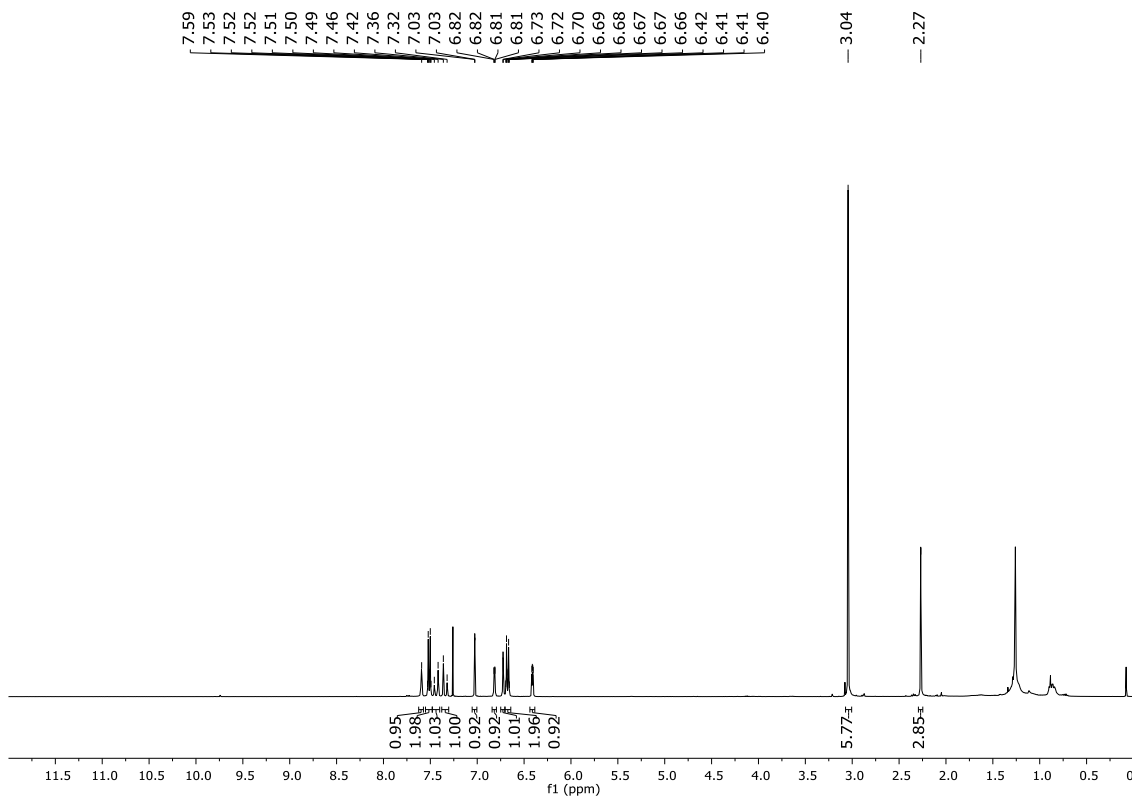


Figure S25. Dimethylamino-BODIPY 5a: $^1\text{H-NMR}$ (400 MHz, CDCl_3).

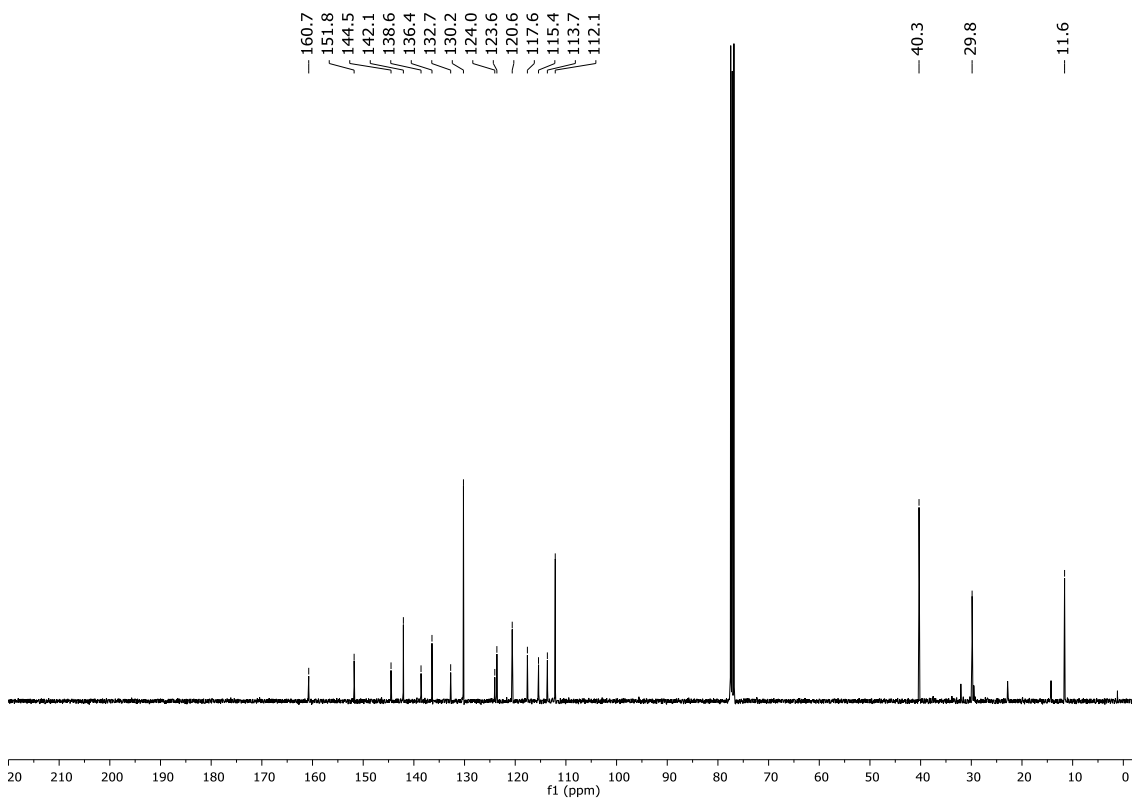


Figure S26. Dimethylamino-BODIPY 5a: $^{13}\text{C-NMR}$ (100.6 MHz, CDCl_3).

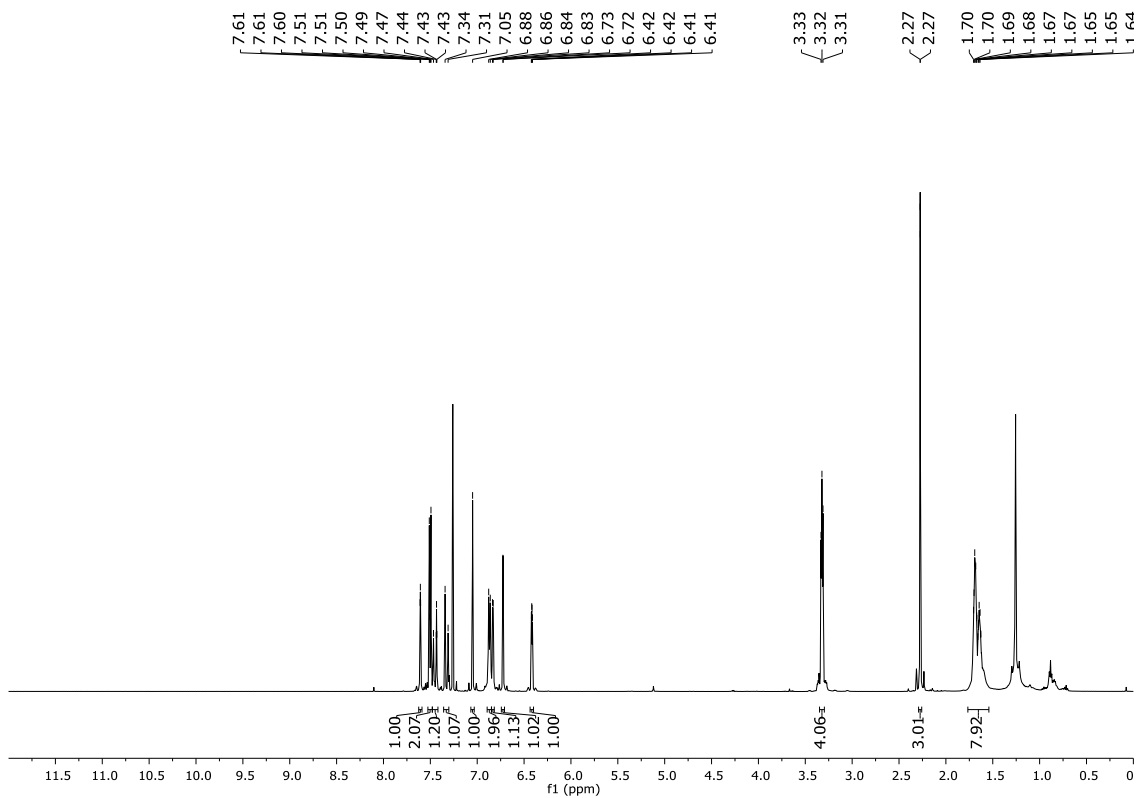


Figure S27. Piperidinyl-BODIPY **5b**: $^1\text{H-NMR}$ (500 MHz, CDCl_3).

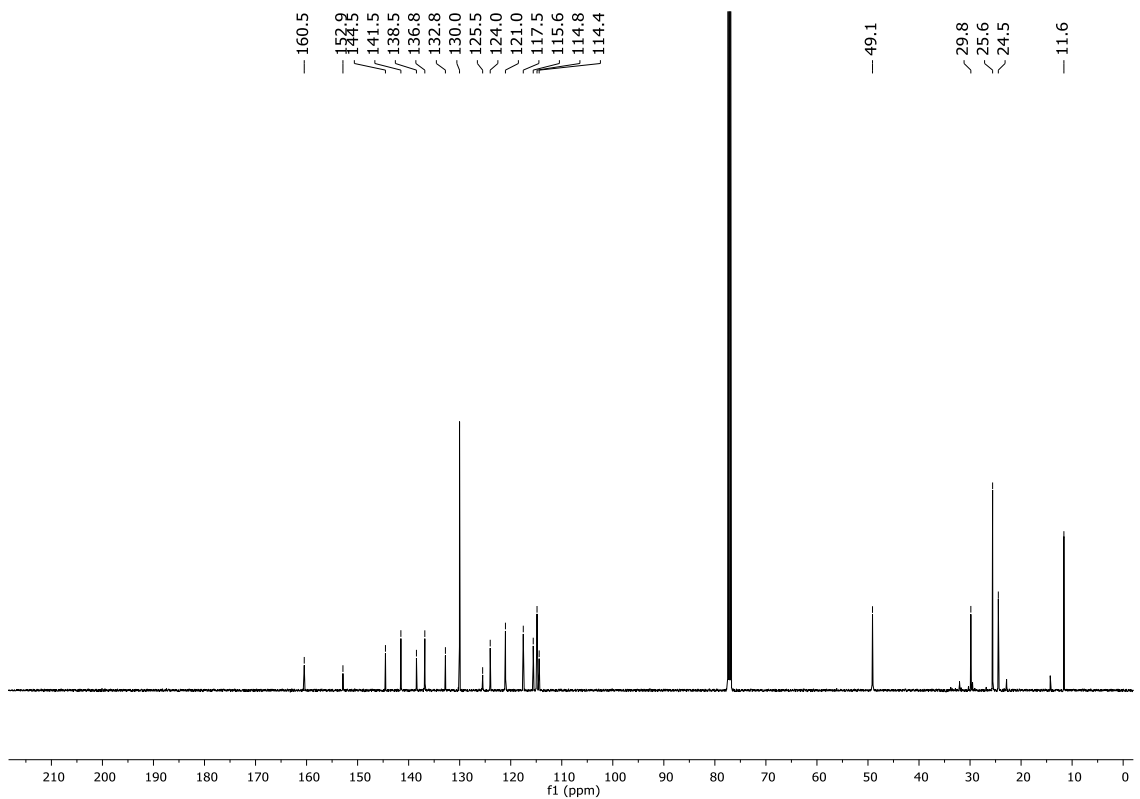


Figure S28. Piperidinyl-BODIPY **5b**: $^{13}\text{C-NMR}$ (125.6 MHz, CDCl_3).

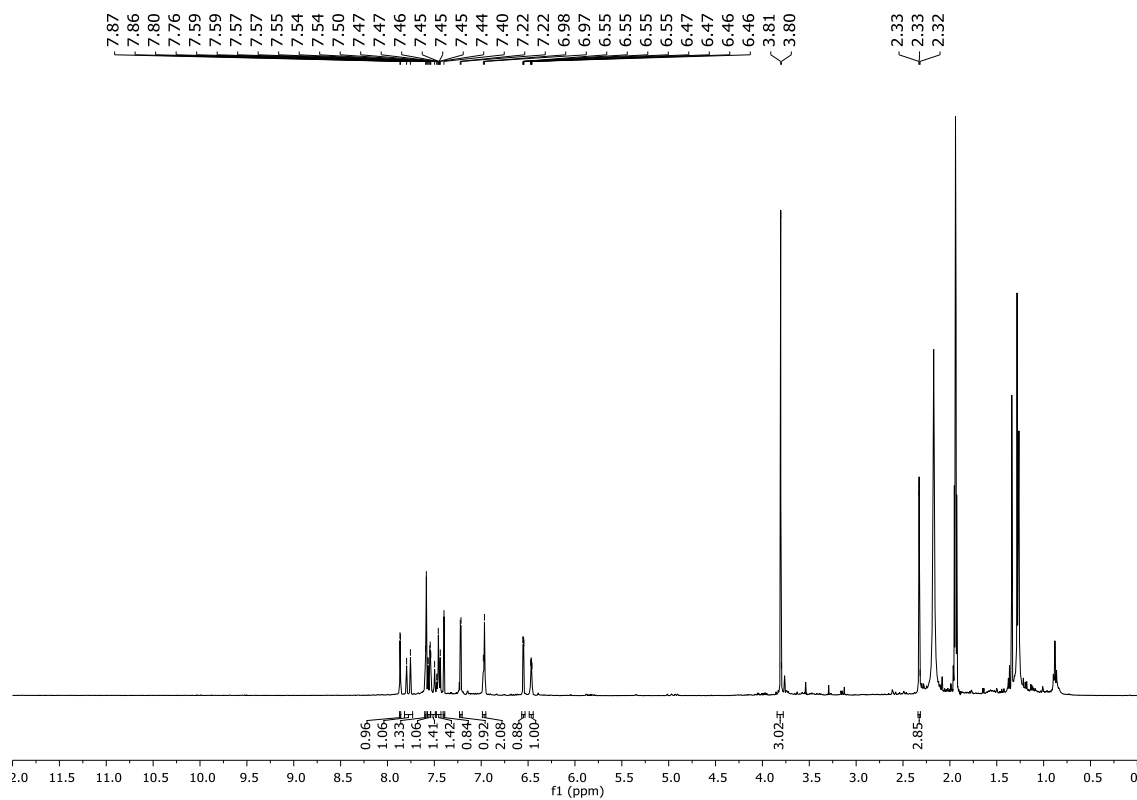


Figure S29. Indacenyl-BODIPY 5c: $^1\text{H-NMR}$ (400 MHz, CD_3CN).

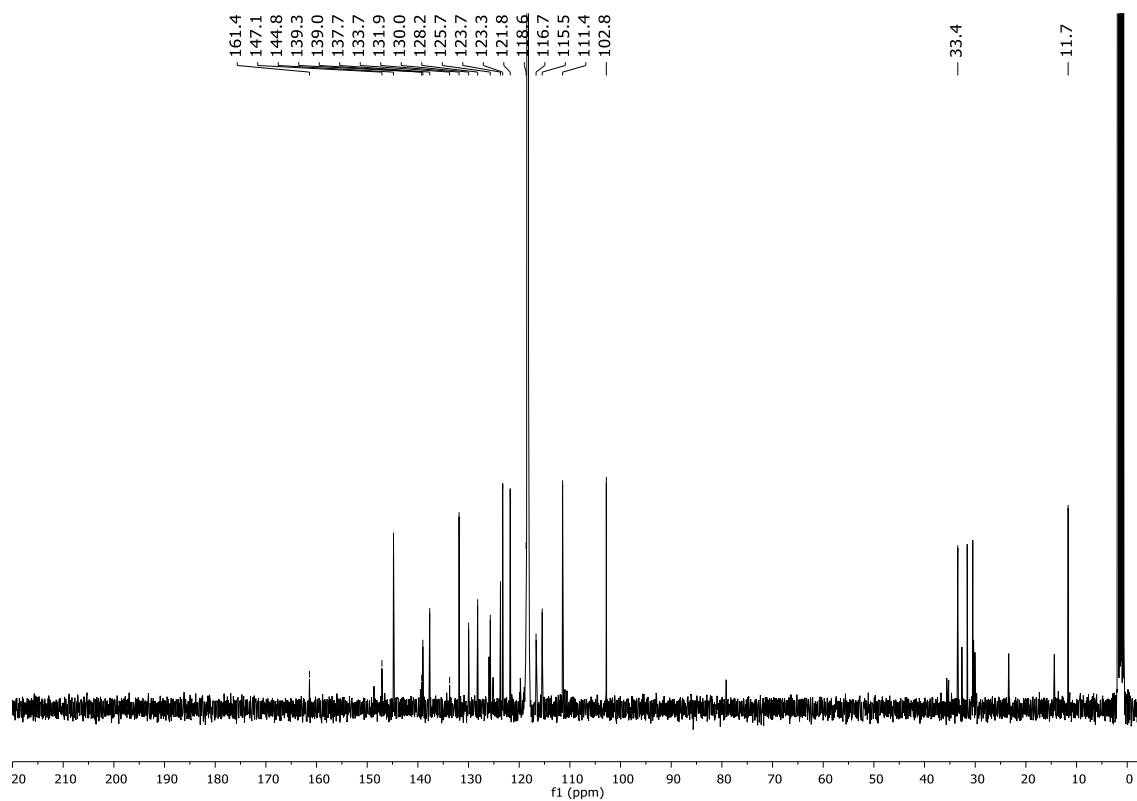


Figure S30. Indacenyl-BODIPY 5c: $^{13}\text{C-NMR}$ (100.6 MHz, CD_3CN).

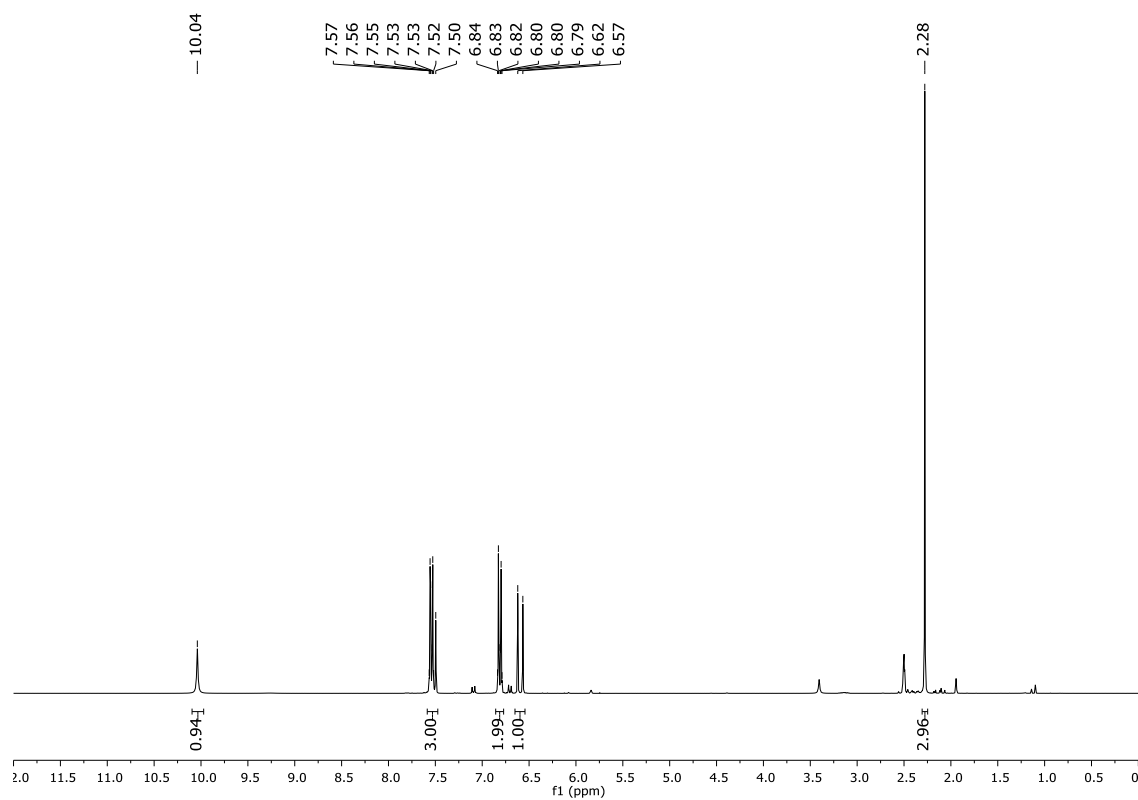


Figure S31. But-3-en-2-one **7a**: $^1\text{H-NMR}$ (300 MHz, DMSO-d_6).

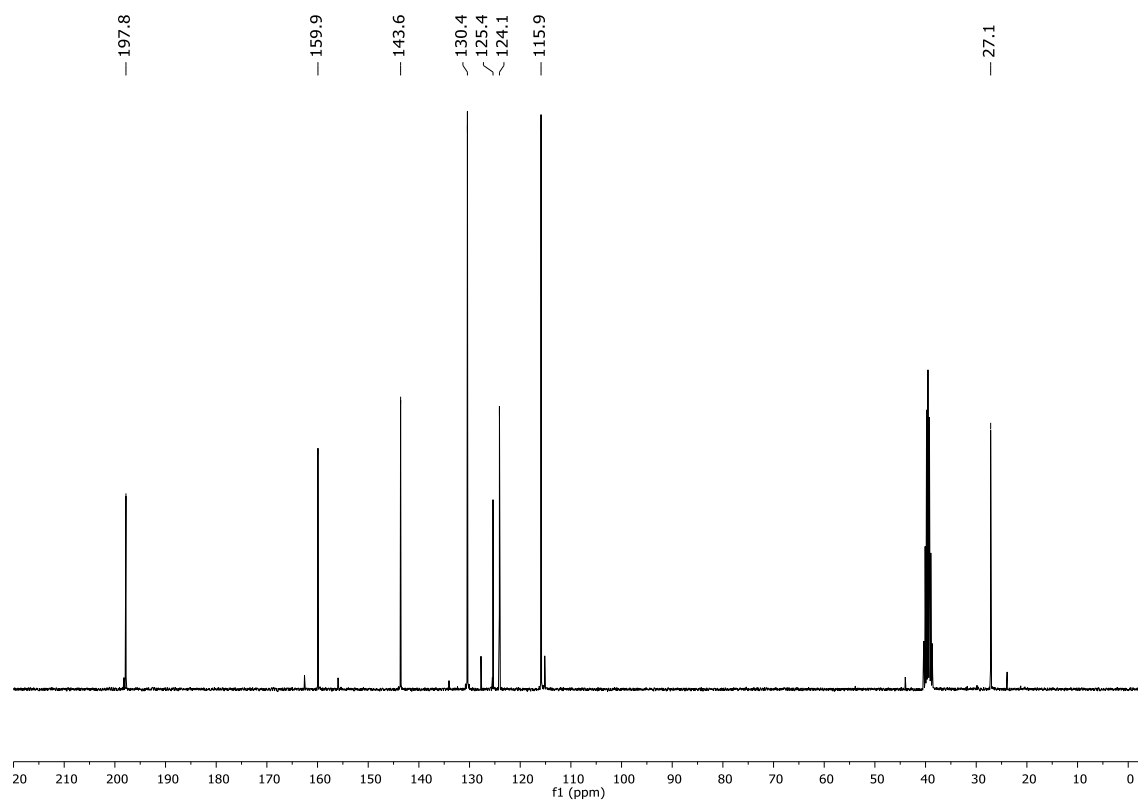


Figure S32. But-3-en-2-one **7a**: $^{13}\text{C-NMR}$ (75.5 MHz, DMSO-d_6).

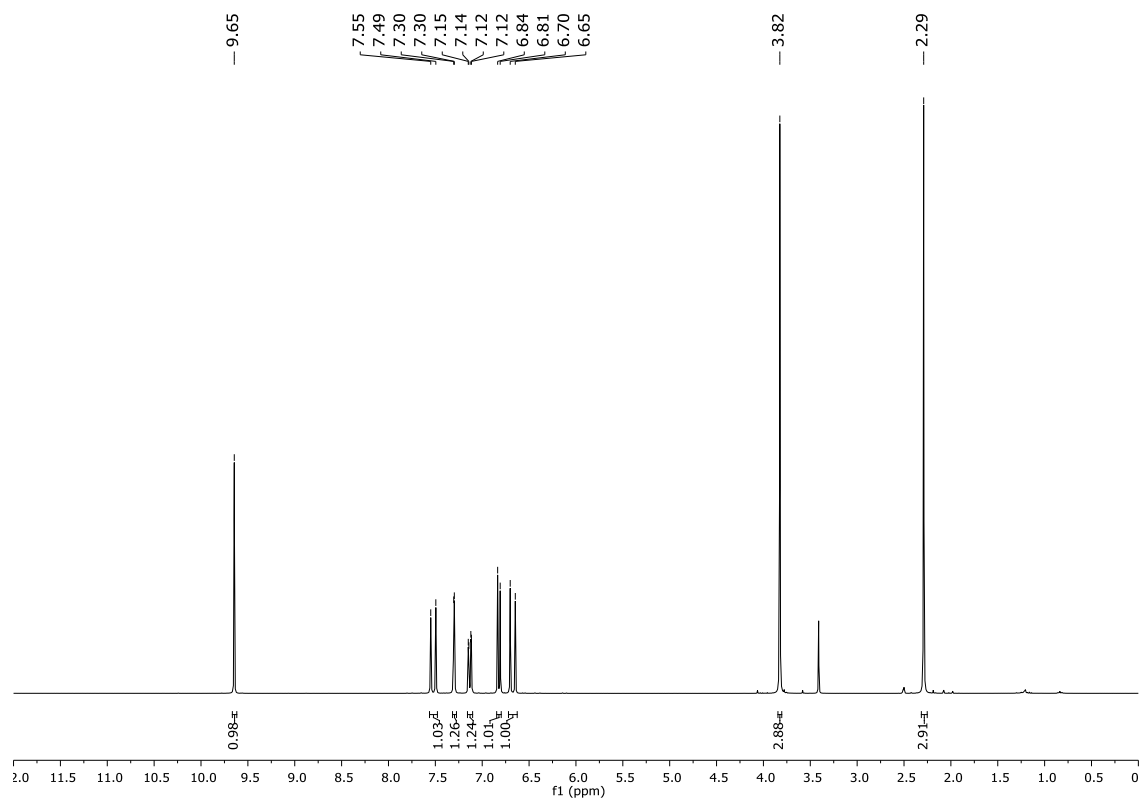


Figure S33. But-3-en-2-one **7b**: $^1\text{H-NMR}$ (300 MHz, DMSO-d_6).

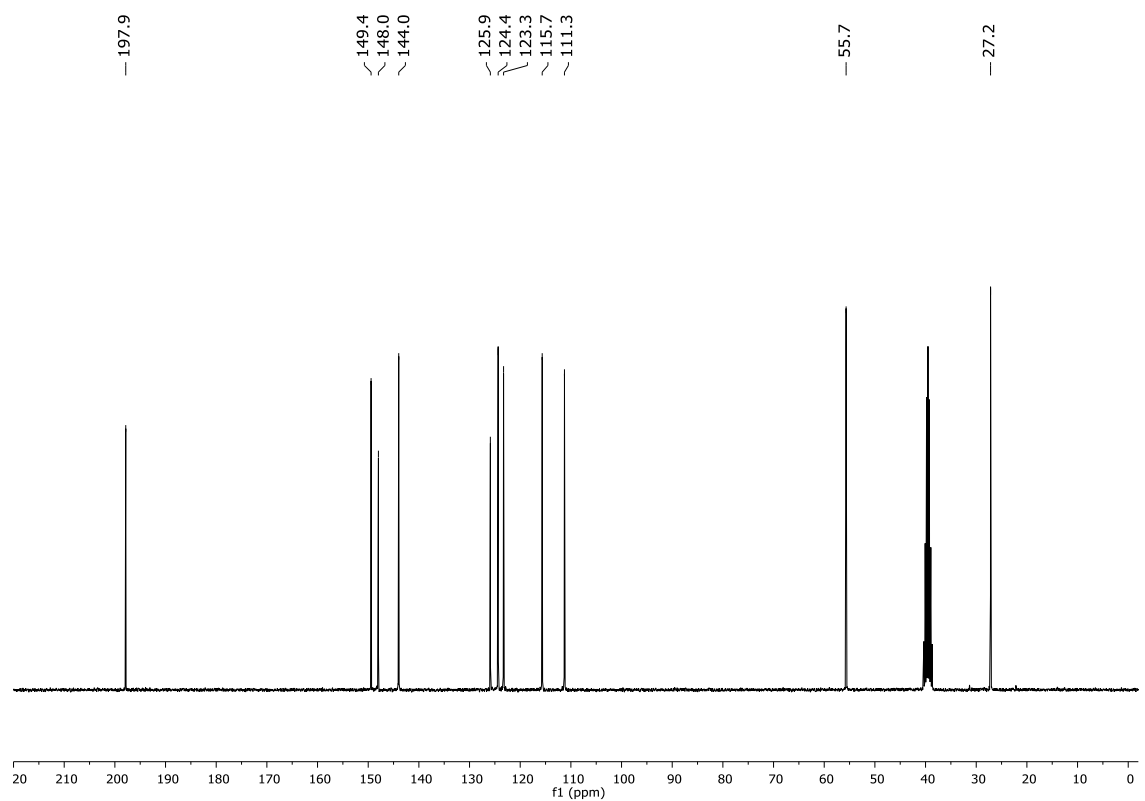


Figure S34. But-3-en-2-one **7b**: $^{13}\text{C-NMR}$ (75.5 MHz, DMSO-d_6).

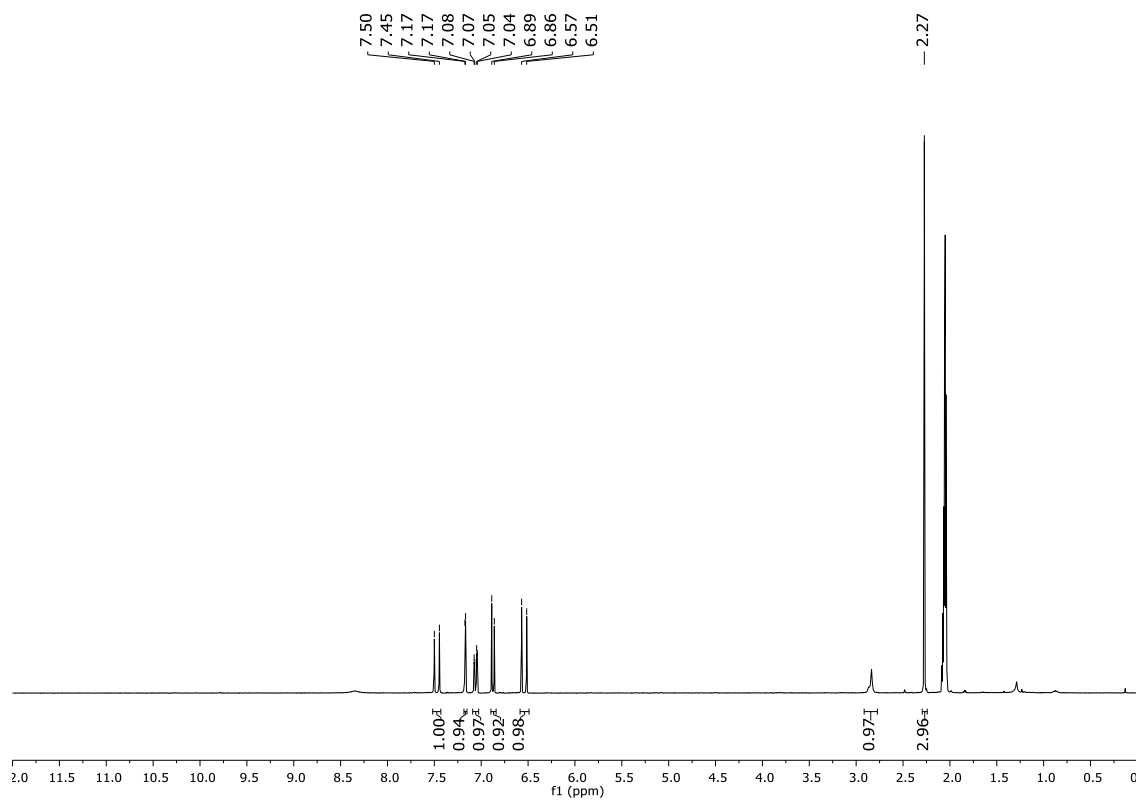


Figure S35. But-3-en-2-one **7c**: $^1\text{H-NMR}$ (300 MHz, acetone- d_6).

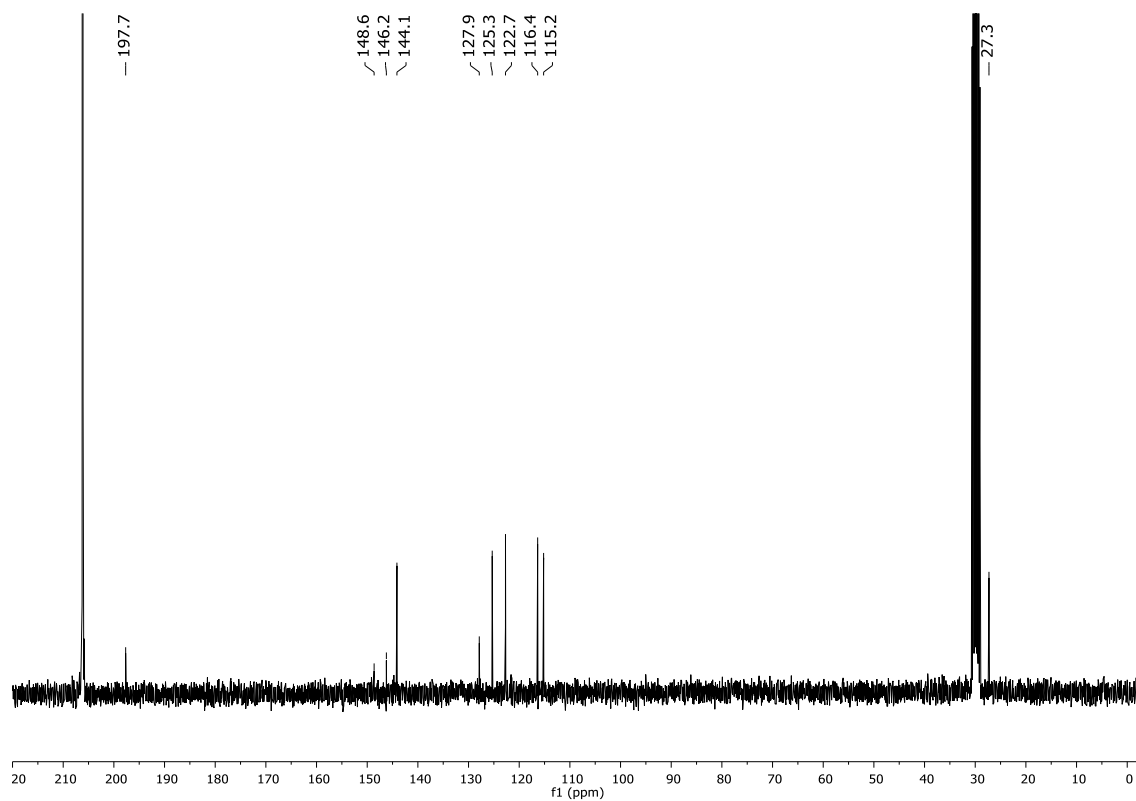


Figure S36. But-3-en-2-one **7c**: $^{13}\text{C-NMR}$ (75.5 MHz, acetone- d_6).

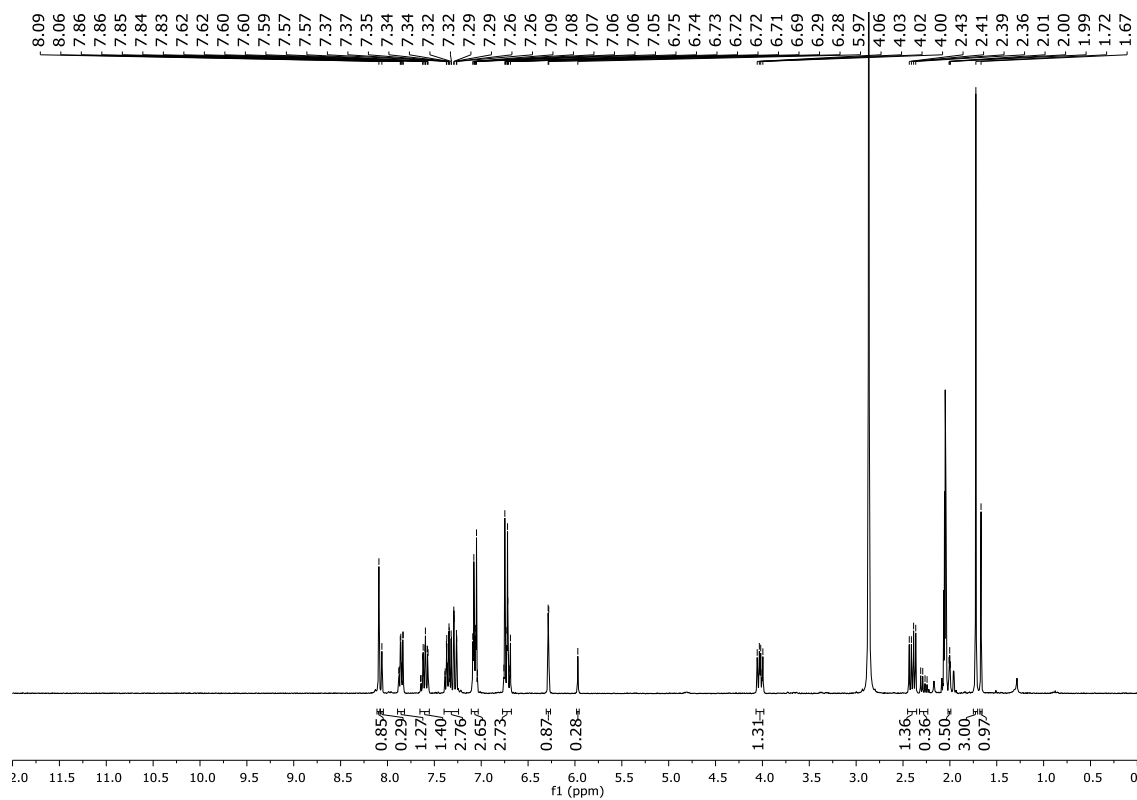


Figure S37. Warfarin derivative **8a**: $^1\text{H-NMR}$ (300 MHz, acetone- d_6).

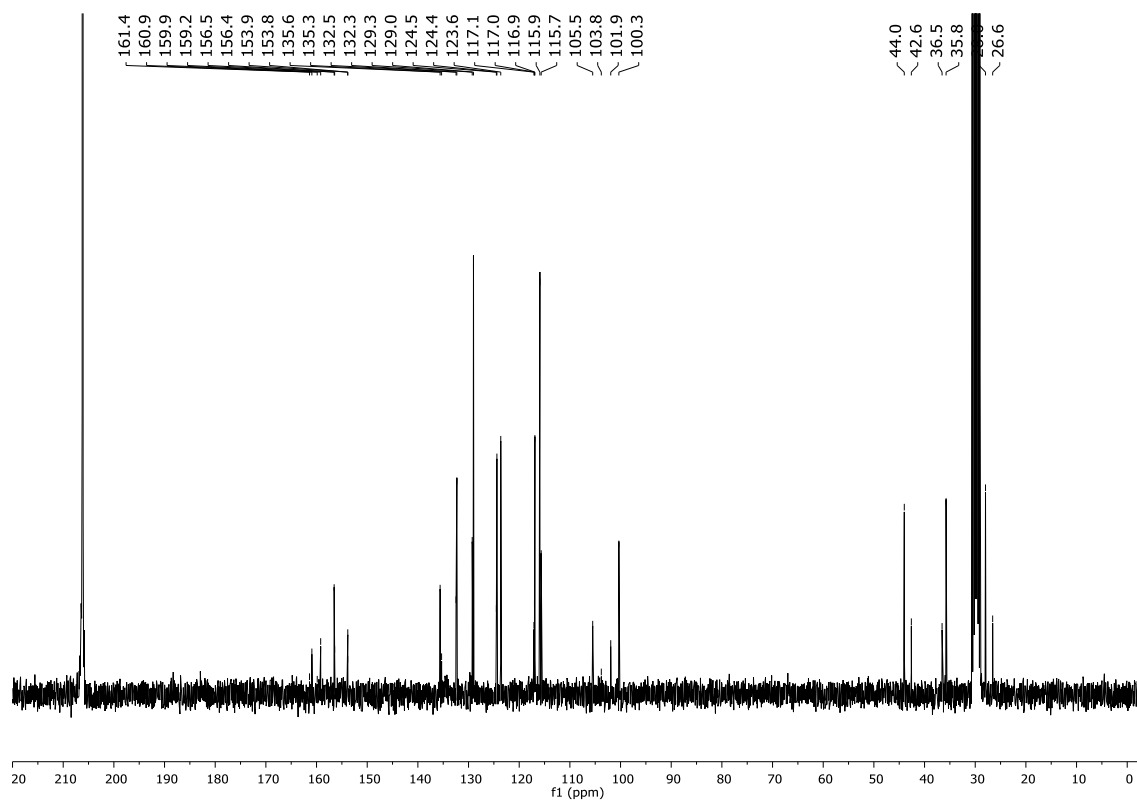


Figure S38. Warfarin derivative **8a**: $^{13}\text{C-NMR}$ (75.5 MHz, acetone- d_6).

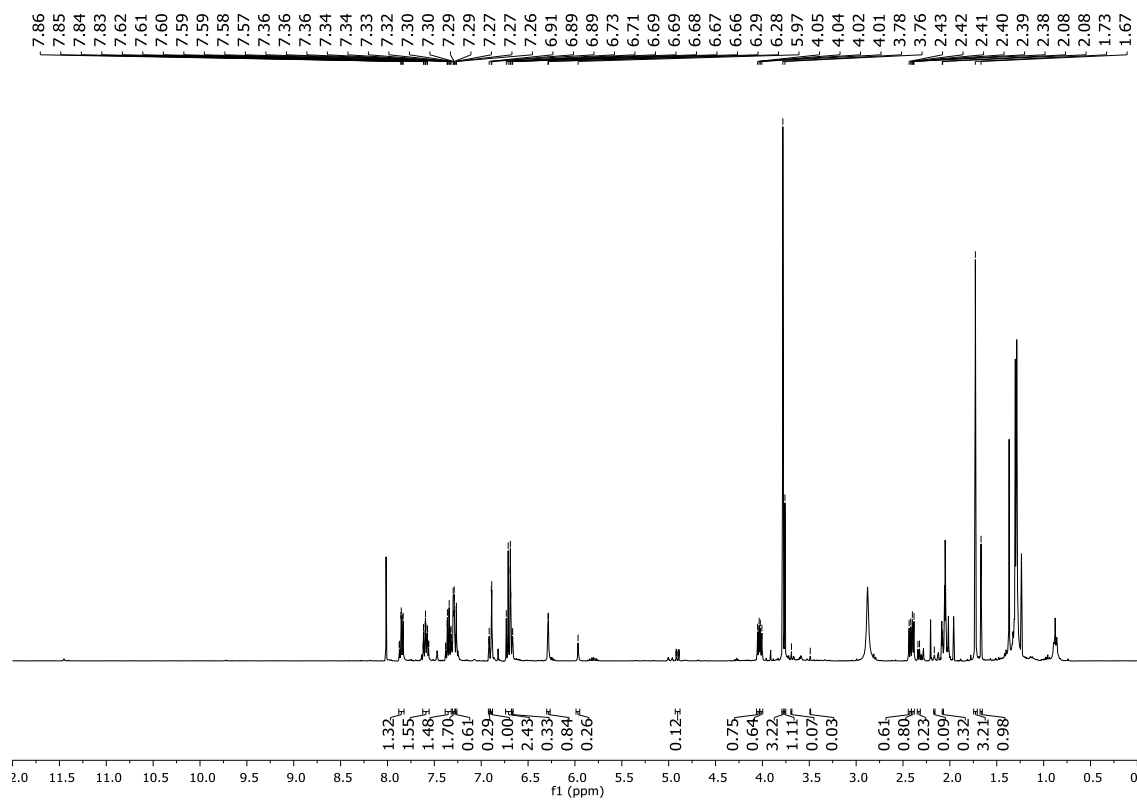


Figure S39. Warfarin derivative **8b**: $^1\text{H-NMR}$ (400 MHz, acetone- d_6).

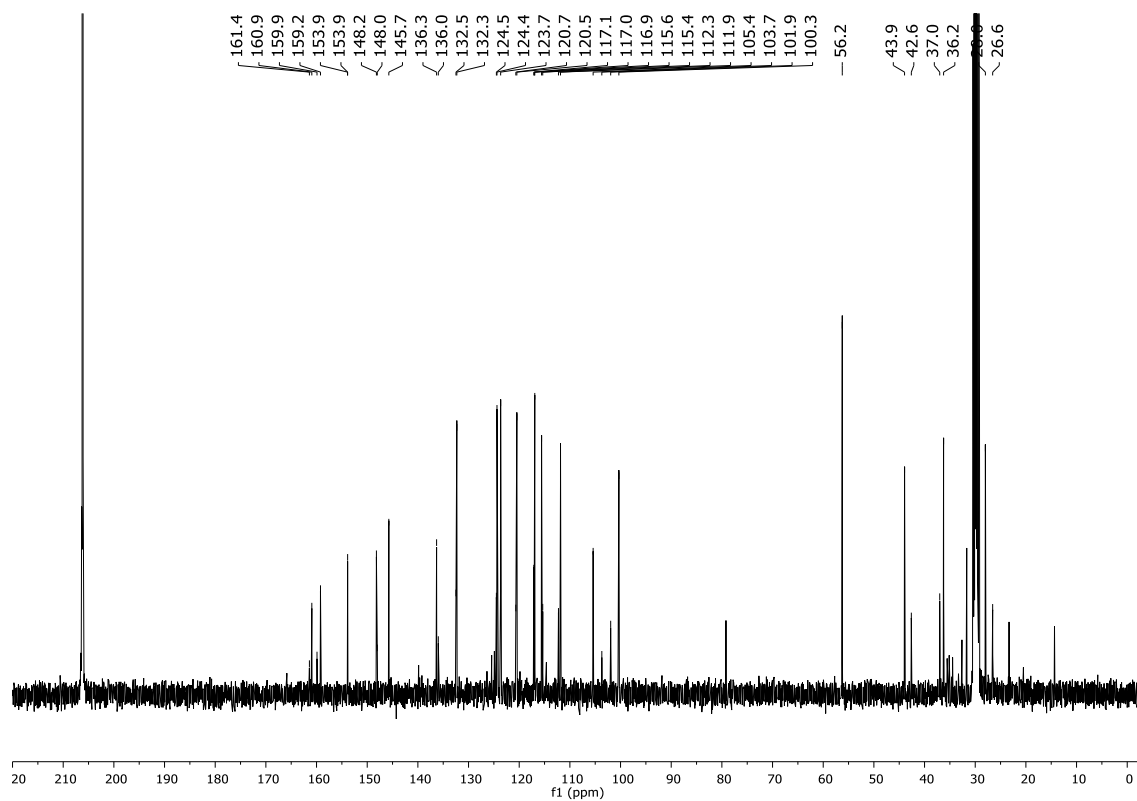


Figure S40. Warfarin derivative **8b**: $^{13}\text{C-NMR}$ (100.6 MHz, acetone- d_6).

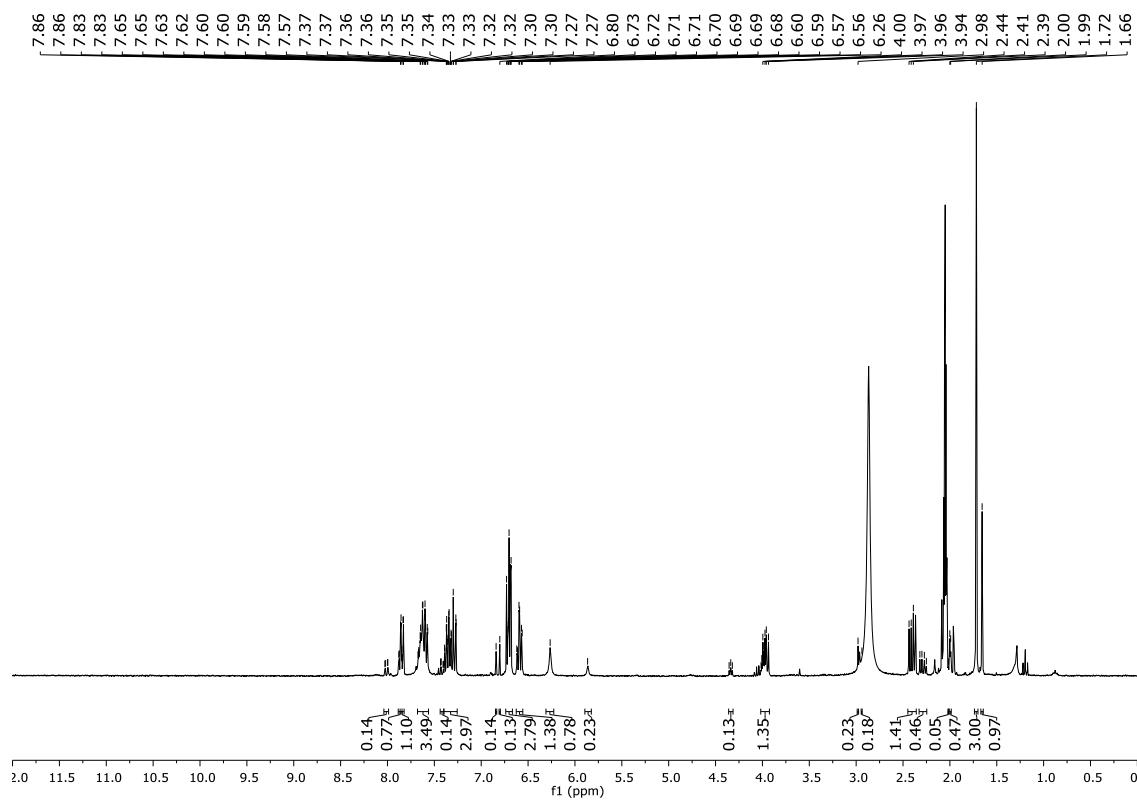


Figure S41. Warfarin derivative **8c**: $^1\text{H-NMR}$ (300 MHz, acetone- d_6).

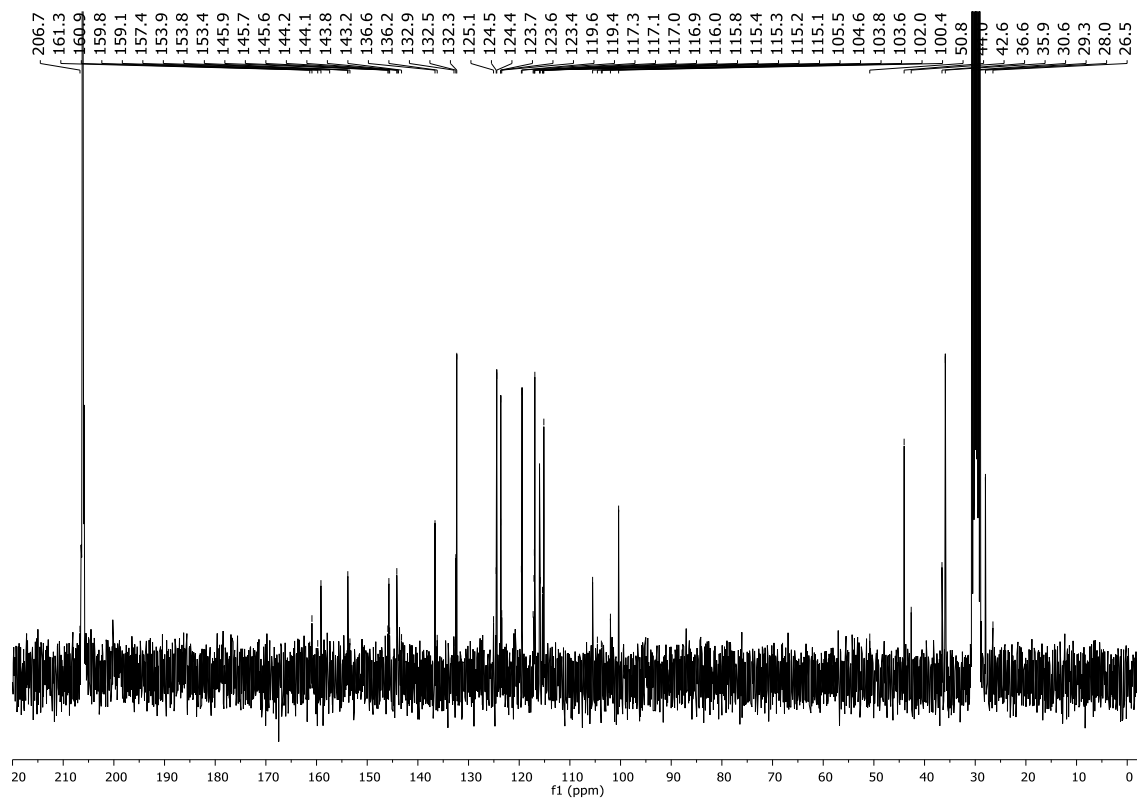


Figure S42. Warfarin derivative **8c**: $^{13}\text{C-NMR}$ (75.5 MHz, acetone- d_6).

IV. X-ray crystallization data for BODIPY derivative 5a

Molecular formula	$C_{20}H_{20}BF_2N_3$
Molecular weight	351.2 $g\text{mol}^{-1}$
Space group name	P -1 (triclinic)
Absorption	$\mu = 0.09\text{ mm}^{-1}$
Crystal size	0.02 x 0.08 x 0.15 mm^3 blue plate
Lattice constant	a = 14.1526(13) \AA $\alpha = 78.797(7)^\circ$
(calculated using	b = 14.7427(13) \AA $\beta = 64.192(7)^\circ$
7683 reflections with	c = 15.9834(14) \AA $\gamma = 65.391(6)^\circ$
$2.6^\circ < \theta < 27.4^\circ$)	V = 2729.2(5) \AA^3 z = 6 F(000) = 1104
Temperature	-80°C
Density	$d_{\text{rön}} = 1.282\text{ gcm}^{-3}$

Data collection

Diffractometer	STOE IPDS 2T
Source	Mo- K_α graphite monochromator

Scan type	ω scans
Scan width	1°

Measuring range	$2^\circ \leq \theta \leq 28^\circ$ $-18 \leq h \leq 18$ $-19 \leq k \leq 19$ $-20 \leq l \leq 17$
-----------------	---

Number of reflections:	
determined	27761
independent	12360 ($R_{\text{int}} = 0.0827$)
overserved	3468 ($ F /\sigma(F) > 4.0$)

Data correction, structure solving and refinement

Correction	Lorentz- and polarisation correction.
Solving	Program: SIR-2004 (direct methods)
Refinement	Program: SHELXL-2014 (full matrix method). 712 refined parameters, weighted refinement: $w = 1/[\sigma^2(F_o^2) + (0.0480 \cdot P)^2]$ where $P = (\text{Max}(F_o^2, 0) + 2 \cdot F_c^2)/3$. H-atoms added geometrically and refined using a riding model, non-H-atoms refined anisotropically.
Discrepancy factor	$wR2 = 0.1835$ ($R1 = 0.0743$ for observed reflections, 0.2617 for all reflections)
Goodness-of-fit	S = 0.92
Maximum variation of parameters	0.001 * e.s.d
Maximum height in differential	
Fourier synthesis	0.32, -0.18 $e\text{\AA}^{-3}$
Remark	structure contains three independent reflections which are almost identical.

Final coordinates and equivalent displacement parameters (Å²)

$$U_{\text{eq}} = (1/3) \sum_{ij} a_i^* a_j^* a_i a_j$$

Atom	X	Y	Z	U_{eq}
C1A	0.4137(5)	-0.0651(4)	0.3780(4)	0.073(3)
C2A	0.3333(5)	-0.0836(4)	0.4597(4)	0.076(4)
C3A	0.3054(4)	-0.0130(4)	0.5219(4)	0.066(3)
C4A	0.3686(4)	0.0465(4)	0.4762(3)	0.055(3)
C5A	0.3751(4)	0.1252(4)	0.5064(3)	0.059(3)
C6A	0.4493(4)	0.1695(4)	0.4495(3)	0.057(3)
C7A	0.4700(4)	0.2505(4)	0.4657(3)	0.061(3)
C8A	0.5553(4)	0.2619(4)	0.3869(3)	0.063(3)
C9A	0.5895(4)	0.1896(4)	0.3214(3)	0.055(3)
N10A	0.4370(3)	0.0121(3)	0.3863(3)	0.059(2)
N11A	0.5238(3)	0.1347(3)	0.3598(2)	0.052(2)
C12A	0.6772(4)	0.1736(4)	0.2296(3)	0.057(3)
C13A	0.7419(4)	0.2278(4)	0.1903(3)	0.059(3)
C14A	0.8284(4)	0.2193(4)	0.0974(3)	0.053(3)
C15A	0.8814(4)	0.2881(4)	0.0626(4)	0.059(3)
C16A	0.9618(4)	0.2849(4)	-0.0263(4)	0.061(3)
C17A	0.9934(4)	0.2111(3)	-0.0872(3)	0.050(3)
C18A	0.9405(4)	0.1415(3)	-0.0540(3)	0.055(3)
C19A	0.8606(4)	0.1454(4)	0.0353(3)	0.057(3)
N20A	1.0736(3)	0.2055(3)	-0.1762(3)	0.062(2)
C21A	1.1000(4)	0.1330(4)	-0.2401(3)	0.068(3)
C22A	1.1419(4)	0.2669(4)	-0.2058(4)	0.075(3)
B23A	0.5289(5)	0.0479(5)	0.3134(4)	0.060(3)
F24A	0.5094(2)	0.0828(2)	0.2331(2)	0.075(2)
F25A	0.6345(2)	-0.0294(2)	0.2907(2)	0.076(2)
C26A	0.4081(4)	0.3069(4)	0.5543(3)	0.081(3)
C1B	0.3885(6)	0.2851(5)	-0.1067(6)	0.120(5)
C2B	0.4765(7)	0.2692(6)	-0.1949(6)	0.132(6)
C3B	0.5124(6)	0.3491(7)	-0.2163(5)	0.128(5)
C4B	0.4470(5)	0.4125(5)	-0.1396(4)	0.084(4)
C5B	0.4472(4)	0.4999(5)	-0.1205(4)	0.082(4)
C6B	0.3779(4)	0.5465(4)	-0.0391(3)	0.068(3)
C7B	0.3711(5)	0.6322(4)	-0.0044(4)	0.072(3)
C8B	0.2895(4)	0.6459(4)	0.0820(4)	0.067(3)
C9B	0.2432(4)	0.5701(4)	0.1031(3)	0.056(3)
N10B	0.3699(4)	0.3707(4)	-0.0740(4)	0.084(3)
N11B	0.2979(3)	0.5100(3)	0.0300(3)	0.059(2)
C12B	0.1562(4)	0.5563(4)	0.1859(3)	0.058(3)
C13B	0.1017(4)	0.6171(4)	0.2601(3)	0.057(3)
C14B	0.0140(4)	0.6103(4)	0.3476(3)	0.057(3)
C15B	-0.0314(4)	0.6797(4)	0.4168(3)	0.061(3)
C16B	-0.1159(4)	0.6750(4)	0.5020(3)	0.065(3)
C17B	-0.1619(4)	0.6017(4)	0.5225(3)	0.059(3)
C18B	-0.1167(4)	0.5324(4)	0.4529(3)	0.059(3)
C19B	-0.0322(4)	0.5373(4)	0.3685(3)	0.057(3)
N20B	-0.2452(4)	0.5981(4)	0.6070(3)	0.076(3)
C21B	-0.2939(5)	0.5231(5)	0.6294(4)	0.086(4)
C22B	-0.2851(5)	0.6658(4)	0.6811(4)	0.088(3)
Atom	X	Y	Z	U_{eq}
B23B	0.2777(5)	0.4189(5)	0.0198(5)	0.070(4)
F24B	0.1700(3)	0.4465(2)	0.0212(2)	0.089(2)
F25B	0.2861(3)	0.3500(2)	0.0930(2)	0.083(2)
C26B	0.4445(5)	0.6923(5)	-0.0573(4)	0.093(4)
C1C	0.2485(5)	0.5379(4)	0.6965(5)	0.084(4)
C2C	0.2166(6)	0.4859(5)	0.7784(5)	0.086(4)

C3C	0.1004(5)	0.5352(4)	0.8256(4)	0.078(4)
C4C	0.0645(5)	0.6147(4)	0.7700(5)	0.071(4)
C5C	-0.0430(4)	0.6884(4)	0.7818(4)	0.068(3)
C6C	-0.0592(4)	0.7570(4)	0.7137(5)	0.065(3)
C7C	-0.1619(5)	0.8341(4)	0.7118(5)	0.070(4)
C8C	-0.1327(5)	0.8773(4)	0.6256(5)	0.076(4)
C9C	-0.0135(5)	0.8302(4)	0.5741(5)	0.068(3)
N10C	0.1579(4)	0.6159(3)	0.6901(4)	0.071(3)
N11C	0.0301(4)	0.7578(3)	0.6291(3)	0.068(3)
C12C	0.0546(5)	0.8484(4)	0.4813(5)	0.073(4)
C13C	0.0142(5)	0.9187(4)	0.4235(5)	0.077(4)
C14C	0.0774(5)	0.9368(4)	0.3262(5)	0.071(4)
C15C	0.0244(5)	1.0161(4)	0.2762(5)	0.083(4)
C16C	0.0827(7)	1.0363(5)	0.1839(6)	0.089(5)
C17C	0.1969(7)	0.9782(5)	0.1367(5)	0.084(5)
C18C	0.2480(6)	0.8985(4)	0.1868(5)	0.086(4)
C19C	0.1905(5)	0.8794(4)	0.2779(5)	0.080(4)
N20C	0.2536(6)	0.9978(4)	0.0461(5)	0.103(4)
C21C	0.3783(8)	0.9575(5)	0.0034(5)	0.132(6)
C22C	0.2007(6)	1.0811(5)	-0.0053(5)	0.123(6)
B23C	0.1549(5)	0.6947(5)	0.6125(6)	0.073(4)
F24C	0.2060(2)	0.7581(2)	0.6137(3)	0.095(2)
F25C	0.2154(3)	0.6499(2)	0.5250(2)	0.091(2)
C26C	-0.2766(4)	0.8596(4)	0.7906(4)	0.086(4)

anisotropic displacement parameters

Atom	U ₁₁	U ₂₂	U ₃₃	U ₁₂	U ₁₃	U ₂₃
C1A	0.075(4)	0.073(4)	0.066(4)	-0.026(3)	-0.028(3)	0.001(3)
C2A	0.073(4)	0.070(4)	0.098(5)	-0.034(3)	-0.043(4)	0.013(4)
C3A	0.054(3)	0.074(4)	0.070(4)	-0.019(3)	-0.032(3)	0.008(3)
C4A	0.043(3)	0.065(3)	0.049(3)	-0.016(3)	-0.017(2)	0.001(3)
C5A	0.049(3)	0.073(4)	0.044(3)	-0.012(3)	-0.016(2)	-0.009(3)
C6A	0.042(3)	0.071(4)	0.044(3)	-0.008(3)	-0.016(2)	-0.003(3)
C7A	0.055(3)	0.067(4)	0.056(3)	-0.012(3)	-0.023(3)	-0.014(3)
C8A	0.051(3)	0.069(4)	0.061(3)	-0.015(3)	-0.019(3)	-0.010(3)
C9A	0.044(3)	0.066(3)	0.048(3)	-0.013(3)	-0.019(2)	-0.003(3)
N10A	0.055(2)	0.067(3)	0.046(2)	-0.017(2)	-0.014(2)	-0.009(2)
N11A	0.040(2)	0.063(3)	0.043(2)	-0.012(2)	-0.013(2)	-0.003(2)
C12A	0.049(3)	0.066(3)	0.047(3)	-0.013(3)	-0.019(2)	-0.001(3)
C13A	0.052(3)	0.068(4)	0.058(3)	-0.023(3)	-0.020(3)	-0.006(3)
C14A	0.045(3)	0.056(3)	0.052(3)	-0.015(2)	-0.018(2)	-0.003(3)
C15A	0.059(3)	0.058(3)	0.069(4)	-0.026(3)	-0.027(3)	-0.007(3)
C16A	0.060(3)	0.058(3)	0.069(4)	-0.032(3)	-0.020(3)	0.000(3)
C17A	0.045(3)	0.049(3)	0.059(3)	-0.020(2)	-0.019(2)	-0.004(2)
Atom	U ₁₁	U ₂₂	U ₃₃	U ₁₂	U ₁₃	U ₂₃
C18A	0.052(3)	0.053(3)	0.057(3)	-0.026(2)	-0.010(3)	-0.004(2)
C19A	0.055(3)	0.060(3)	0.060(3)	-0.030(3)	-0.020(3)	0.003(3)
N20A	0.055(2)	0.064(3)	0.059(3)	-0.031(2)	-0.006(2)	-0.007(2)
C21A	0.065(3)	0.077(4)	0.052(3)	-0.028(3)	-0.010(3)	-0.010(3)
C22A	0.069(3)	0.077(4)	0.081(4)	-0.042(3)	-0.020(3)	0.006(3)
B23A	0.058(4)	0.070(4)	0.046(3)	-0.020(3)	-0.023(3)	0.004(3)
F24A	0.074(2)	0.111(2)	0.048(2)	-0.043(2)	-0.024(1)	0.002(2)
F25A	0.053(2)	0.077(2)	0.074(2)	-0.011(1)	-0.011(1)	-0.018(2)
C26A	0.071(4)	0.091(4)	0.065(4)	-0.017(3)	-0.017(3)	-0.027(3)
C1B	0.116(6)	0.090(5)	0.141(7)	0.021(4)	-0.074(5)	-0.055(5)

C2B	0.110(6)	0.116(7)	0.147(8)	0.017(5)	-0.056(6)	-0.080(6)
C3B	0.089(5)	0.157(8)	0.100(6)	0.015(5)	-0.037(4)	-0.062(6)
C4B	0.053(3)	0.103(5)	0.063(4)	0.005(4)	-0.020(3)	-0.017(4)
C5B	0.056(3)	0.092(5)	0.073(4)	-0.003(3)	-0.025(3)	-0.007(4)
C6B	0.042(3)	0.089(4)	0.044(3)	-0.006(3)	-0.014(3)	0.005(3)
C7B	0.065(3)	0.077(4)	0.083(4)	-0.029(3)	-0.040(3)	0.015(3)
C8B	0.057(3)	0.069(4)	0.068(4)	-0.024(3)	-0.022(3)	0.007(3)
C9B	0.052(3)	0.059(3)	0.051(3)	-0.019(3)	-0.020(3)	0.003(3)
N10B	0.080(3)	0.077(4)	0.087(4)	0.001(3)	-0.048(3)	-0.021(3)
N11B	0.053(2)	0.071(3)	0.044(2)	-0.018(2)	-0.016(2)	0.000(2)
C12B	0.059(3)	0.057(3)	0.055(3)	-0.023(3)	-0.020(3)	0.002(3)
C13B	0.058(3)	0.058(3)	0.060(3)	-0.025(3)	-0.023(3)	-0.002(3)
C14B	0.057(3)	0.057(3)	0.057(3)	-0.021(3)	-0.022(3)	-0.003(3)
C15B	0.072(3)	0.059(3)	0.061(3)	-0.028(3)	-0.030(3)	-0.005(3)
C16B	0.070(3)	0.071(4)	0.054(3)	-0.022(3)	-0.025(3)	-0.015(3)
C17B	0.056(3)	0.067(4)	0.056(3)	-0.022(3)	-0.024(3)	-0.004(3)
C18B	0.059(3)	0.063(3)	0.055(3)	-0.024(3)	-0.019(3)	-0.010(3)
C19B	0.066(3)	0.062(3)	0.043(3)	-0.023(3)	-0.019(3)	-0.010(2)
N20B	0.072(3)	0.095(4)	0.052(3)	-0.032(3)	-0.013(2)	-0.008(3)
C21B	0.084(4)	0.100(5)	0.063(4)	-0.038(4)	-0.017(3)	0.004(3)
C22B	0.079(4)	0.107(5)	0.058(3)	-0.017(3)	-0.017(3)	-0.027(3)
B23B	0.056(4)	0.073(5)	0.068(4)	-0.006(3)	-0.030(3)	-0.003(4)
F24B	0.076(2)	0.092(2)	0.103(2)	-0.018(2)	-0.043(2)	-0.024(2)
F25B	0.098(2)	0.066(2)	0.092(2)	-0.030(2)	-0.046(2)	0.002(2)
C26B	0.081(4)	0.110(5)	0.097(5)	-0.057(4)	-0.037(4)	0.032(4)
C1C	0.085(4)	0.057(4)	0.124(6)	-0.012(4)	-0.063(4)	-0.014(4)
C2C	0.097(5)	0.055(4)	0.119(5)	-0.008(4)	-0.069(4)	-0.014(4)
C3C	0.088(4)	0.062(4)	0.101(5)	-0.020(3)	-0.056(4)	-0.013(4)
C4C	0.069(4)	0.055(4)	0.103(5)	-0.019(3)	-0.048(4)	-0.011(3)
C5C	0.073(4)	0.057(4)	0.093(4)	-0.025(3)	-0.041(3)	-0.019(3)
C6C	0.062(3)	0.045(3)	0.106(5)	-0.017(3)	-0.051(4)	-0.005(3)
C7C	0.068(4)	0.060(4)	0.102(5)	-0.027(3)	-0.047(4)	-0.009(3)
C8C	0.065(4)	0.063(4)	0.119(5)	-0.020(3)	-0.054(4)	-0.009(4)
C9C	0.070(4)	0.055(4)	0.103(5)	-0.025(3)	-0.052(4)	-0.006(3)
N10C	0.070(3)	0.048(3)	0.112(4)	-0.013(2)	-0.056(3)	-0.008(3)
N11C	0.065(3)	0.058(3)	0.097(3)	-0.022(2)	-0.046(3)	-0.005(3)
C12C	0.080(4)	0.056(4)	0.107(5)	-0.029(3)	-0.056(4)	-0.001(3)
C13C	0.082(4)	0.052(4)	0.124(5)	-0.026(3)	-0.062(4)	-0.004(4)
C14C	0.080(4)	0.049(3)	0.109(5)	-0.021(3)	-0.063(4)	0.002(3)
C15C	0.091(4)	0.049(4)	0.144(6)	-0.026(3)	-0.083(5)	0.006(4)
C16C	0.123(6)	0.058(4)	0.138(6)	-0.046(4)	-0.096(5)	0.022(4)
C17C	0.118(6)	0.068(4)	0.108(5)	-0.039(4)	-0.083(5)	0.016(4)
C18C	0.108(5)	0.062(4)	0.107(5)	-0.022(4)	-0.070(5)	0.005(4)
C19C	0.092(5)	0.058(4)	0.100(5)	-0.015(3)	-0.059(4)	-0.003(4)
N20C	0.142(5)	0.091(4)	0.120(5)	-0.052(4)	-0.093(5)	0.029(4)
C21C	0.182(9)	0.101(6)	0.098(6)	-0.028(6)	-0.065(6)	-0.002(5)
C22C	0.188(7)	0.099(6)	0.144(6)	-0.071(5)	-0.126(6)	0.051(5)
Atom	U ₁₁	U ₂₂	U ₃₃	U ₁₂	U ₁₃	U ₂₃
B23C	0.062(4)	0.055(4)	0.117(6)	-0.019(3)	-0.046(4)	-0.011(4)
F24C	0.078(2)	0.076(2)	0.162(3)	-0.036(2)	-0.071(2)	0.008(2)
F25C	0.087(2)	0.075(2)	0.100(3)	-0.018(2)	-0.037(2)	-0.008(2)
C26C	0.075(4)	0.071(4)	0.121(5)	-0.021(3)	-0.051(4)	-0.010(4)

Final coordinates and isotropic displacement parameters of H-atoms(Å²)

Atom	X	Y	Z	U _{iso}
H1A	0.44852	-0.10200	0.32273	0.087
H2A	0.30321	-0.13373	0.47116	0.092
H3A	0.25239	-0.00654	0.58468	0.080
H5A	0.32696	0.14864	0.56784	0.070
H8A	0.58713	0.31047	0.37688	0.076
H12A	0.69014	0.12124	0.19460	0.069
H13A	0.72954	0.27758	0.22780	0.071
H15A	0.86095	0.33952	0.10219	0.071
H16A	0.99610	0.33291	-0.04649	0.074
H18A	0.96034	0.09073	-0.09407	0.066
H19A	0.82641	0.09725	0.05560	0.068
H21A	1.02973	0.13583	-0.24039	0.102
H21B	1.13996	0.06606	-0.22051	0.102
H21C	1.14826	0.14780	-0.30273	0.102
H22A	1.17926	0.25533	-0.16343	0.112
H22B	1.09285	0.33749	-0.20486	0.112
H22C	1.19924	0.24897	-0.26903	0.112
H26A	0.41166	0.25990	0.60649	0.121
H26B	0.32880	0.34463	0.56333	0.121
H26C	0.44325	0.35302	0.55123	0.121
H1B	0.34839	0.24215	-0.07499	0.144
H2B	0.50654	0.21396	-0.23353	0.158
H3B	0.57036	0.35870	-0.27230	0.154
H5B	0.49823	0.52797	-0.16656	0.099
H8B	0.26619	0.69743	0.12262	0.080
H12B	0.13474	0.50197	0.18986	0.069
H13B	0.12494	0.67099	0.25287	0.069
H15B	-0.00334	0.73125	0.40487	0.073
H16B	-0.14359	0.72267	0.54776	0.078
H18B	-0.14522	0.48117	0.46438	0.070
H19B	-0.00408	0.48940	0.32283	0.068
H21D	-0.35536	0.53523	0.69143	0.130
H21E	-0.23541	0.45686	0.62841	0.130
H21F	-0.32383	0.52643	0.58348	0.130
H22D	-0.22268	0.65453	0.69864	0.132
H22E	-0.34695	0.65337	0.73519	0.132
H22F	-0.31235	0.73490	0.65935	0.132
H26D	0.45842	0.71843	-0.01370	0.139
H26E	0.40576	0.74796	-0.09030	0.139
H26F	0.51681	0.64946	-0.10225	0.139
H1C	0.32377	0.52132	0.65089	0.101
Atom	X	Y	Z	U _{iso}
H2C	0.26445	0.42758	0.79874	0.103
H3C	0.05428	0.51757	0.88506	0.094
H5C	-0.10574	0.69023	0.83871	0.082
H8C	-0.18350	0.93033	0.60329	0.091
H12C	0.13335	0.80897	0.45817	0.087
H13C	-0.06367	0.96049	0.44948	0.092
H15C	-0.05327	1.05668	0.30660	0.099
H16C	0.04459	1.09023	0.15237	0.107
H18C	0.32501	0.85652	0.15623	0.104
H19C	0.22897	0.82518	0.30905	0.096
H21G	0.40713	0.88614	0.01832	0.199
H21H	0.40660	0.99253	0.02756	0.199
H21I	0.40426	0.96709	-0.06423	0.199

H22G	0.25441	1.07998	-0.07007	0.184
H22H	0.17906	1.14400	0.02285	0.184
H22I	0.13315	1.07551	-0.00323	0.184
H26G	-0.27159	0.86952	0.84714	0.129
H26H	-0.30299	0.80497	0.80089	0.129
H26I	-0.33016	0.92101	0.77500	0.129

V. References

- [1] G. R. Fulmer, A. J. Miller, N. H. Sherden, H. E. Gottlieb, A. Nudelman, B. M. Stoltz, J. E. Bercaw, K. I. Goldberg, *Organometallics* **2010**, *29*, 2176-2179.
- [2] J.-S. Lee, N.-y. Kang, Y. K. Kim, A. Samanta, S. Feng, H. K. Kim, M. Vendrell, J. H. Park, Y.-T. Chang, *J. Am. Chem. Soc.* **2009**, *131*, 10077-10082.
- [3] X. Li, S. J. Qian, Q. J. He, B. Yang, J. Li, Y. Z. Hu, *Org. Biomol. Chem.* **2010**, *8*, 3627-3630.
- [4] J. C. Er, M. Vendrell, M. K. Tang, D. Zhai, Y.-T. Chang, *ACS Comb. Sci.* **2013**, *15*, 452-457.
- [5] P.-Y. Chen, Y.-H. Wu, M.-H. Hsu, T.-P. Wang, E.-C. Wang, *Tetrahedron* **2013**, *69*, 653-657.
- [6] T. Chuprajob, C. Changtam, R. Chokchaisiri, W. Chunglok, N. Sornkaew, A. Suksamrarn, *Bioorg. Med. Chem. Lett.* **2014**, *24*, 2839-2844.
- [7] A. Baranovsky, B. Schmitt, D. J. Fowler, B. Schneider, *Synth. Commun.* **2003**, *33*, 1019-1045.
- [8] N. Halland, T. Hansen, K. A. Jørgensen, *Angew. Chem.* **2003**, *115*, 5105-5107.
- [9] M. Ikawa, M. A. Stahmann, K. P. Link, *J. Am. Chem. Soc.* **1944**, *66*, 902-906.
- [10] S. C. Gill, P. H. Von Hippel, *Anal. Biochem.* **1989**, *182*, 319-326.
- [11] GraphPad Software, San Diego California USA, www.graphpad.com.
- [12] P. Job, *Ann. Chim. Appl.* **1928**, *9*, 113-203.
- [13] C. Y. Huang, *Methods Enzymol.* **1982**, *87*, 509-525.
- [14] S. Curry, H. Mandelkow, P. Brick, N. Franks, *Nat. Struct. Biol.* **1998**, *5*, 827-835.
- [15] W. Kabsch, *Acta Crystallogr. Sect. D: Biol. Crystallogr.* **2010**, *66*, 125-132.
- [16] P. Evans, *Acta Crystallogr. Sect. D: Biol. Crystallogr.* **2006**, *62*, 72-82.
- [17] I. Tickle, C. Flensburg, P. Keller, W. Paciorek, A. Sharff, C. Vonrhein, G. Bricogne, *Cambridge, United Kingdom: Global Phasing Ltd* **2017**.
- [18] C. Vonrhein, C. Flensburg, P. Keller, A. Sharff, O. Smart, W. Paciorek, T. Womack, G. Bricogne, *Acta Crystallogr. Sect. D: Biol. Crystallogr.* **2011**, *67*, 293-302.
- [19] A. J. McCoy, R. W. Grosse-Kunstleve, P. D. Adams, M. D. Winn, L. C. Storoni, R. J. Read, *J. Appl. Crystallogr.* **2007**, *40*, 658-674.
- [20] P. Emsley, B. Lohkamp, W. G. Scott, K. Cowtan, *Acta Crystallogr. Sect. D: Biol. Crystallogr.* **2010**, *66*, 486-501.
- [21] G. Bricogne, E. Blanc, M. Brandl, C. Flensburg, P. Keller, W. Paciorek, P. Roversi, A. Sharff, O. Smart, C. Vonrhein, *Cambridge, United Kingdom: Global Phasing Ltd* **2011**.
- [22] X. M. He, D. C. Carter, *Nature* **1992**, *358*, 209-215.
- [23] R. Abel, T. Young, R. Farid, B. J. Berne, R. A. Friesner, *J. Am. Chem. Soc.* **2008**, *130*, 2817-2831.

VI. Author Contributions

S.M.P. and T.O. designed the study and supervised the project. L.W. carried out the synthesis and characterization of the fluorescent derivatives and performed the biochemical experiments. J.R. performed the Biosensor Experiments. H.S. carried out the crystallization of sulfasalazine and HSA. H.M. performed the modelling and simulation studies. S.M.P., T.O., L.W., M.W. and H.M. discussed the data and wrote the paper.